

A unified framework for fitting Bayesian semiparametric models to arbitrarily censored spatial survival data

Haiming Zhou

Division of Statistics, Northern Illinois University

and

Timothy Hanson

Department of Statistics, University of South Carolina

July 2, 2022

Abstract

A comprehensive, unified approach to modeling arbitrarily censored spatial survival data is presented for the three most commonly-used semiparametric models: proportional hazards, proportional odds, and accelerated failure time. Unlike many other approaches, all manner of censored survival times are simultaneously accommodated including uncensored, interval censored, current-status, left and right censored, and mixtures of these. Left-truncated data are also accommodated leading to models for time-dependent covariates. Both georeferenced (location observed exactly) and areally observed (location known up to a geographic unit such as a county) spatial locations are handled; formal variable selection makes model selection especially easy. Model fit is assessed with conditional Cox-Snell residual plots, and model choice is carried out via LPML and DIC. Baseline survival is modeled with a novel transformed Bernstein polynomial prior. All models are fit via a new function which calls efficient compiled C++ in the R package `spBayesSurv`. The methodology is broadly illustrated with simulations and real data applications. An important finding is that proportional odds and accelerated failure time models often fit significantly better than the commonly-used proportional hazards model. Supplementary materials are available.

Keywords: Bernstein polynomial; Interval censored data; Spatial frailty models; Variable selection

1 Introduction

Spatial location often plays a key role in prediction, serving as a proxy for unmeasured regional characteristics such as socioeconomic status, access and quality of healthcare, pollution, etc. Spatial models use location both as a means for blocking leading to more precisely estimated non-spatial risk factors, but also as a focal point of inference in its own right, for example to delineate regional “hot spots” or outbreaks that merit closer attention or increased resources. Literature on the spatial analysis of time-to-event data related to human health has flourished over the last decade, including data on leukemia survival (Henderson et al., 2002), infant/childhood mortality (Banerjee et al., 2003; Kneib, 2006), coronary artery bypass grafting (Hennerfeind et al., 2006), asthma (Li and Ryan, 2002; Li and Lin, 2006), breast cancer (Zhao and Hanson, 2011; Hanson et al., 2012; Zhou et al., 2015), mortality due to air pollution (Jerrett et al., 2013), colorectal cancer survival (Liu et al., 2014), smoking cessation (Pan et al., 2014), HIV/AIDS patients (Martins et al., 2016), time to tooth loss (Schnell et al., 2015), and many others. Spatial survival models have also been used in other important areas such as the study of political event processes (Darmofal, 2009), agricultural mildew outbreaks (Ojiambo and Kang, 2013), forest fires (Morin, 2014), pine trees (Li et al., 2015a), health and pharmaceutical firms (Arbia et al., 2016), and emergency service response times (Taylor, 2016) to name a few.

A shortcoming of all twenty papers referenced above is the use of the proportional hazards (PH) model as the only means for obtaining inference; competing models that might provide better fit, such as accelerated failure time (AFT) or proportional odds (PO) models are not considered. There are a few papers using models alternative to PH in a spatial context, e.g. Diva et al. (2008), Zhao et al. (2009), Wang et al. (2012), and Li et al. (2015b) but they tend to be limited in scope. For example, all four of these latter papers only consider areal data, do not employ variable selection or allow time-dependent covariates, and are developed for right censored data only. In general the literature is fragmented in that a method for variable selection in the PH model for non-spatial right censored data will comprise one

paper; another paper may extend the PO model for fitting current status data to general interval censored data, but does not include variable selection, spatial frailties, etc. In this paper, a broadly inclusive, comprehensive treatment of three competing, highly interpretable semiparametric survival models, PH, PO, and AFT, is developed and illustrated on several real and simulated data sets. This work represents the culmination of a great deal of effort tying together many disparate ideas and methodologies in the literature as well as developing an efficient approach to mixed interval censored, observed exactly, and truncated data that can be widely applied to different semiparametric models.

A major finding of this work is that *the survival model itself* plays the most important role in prediction and model fit. Dozens if not hundreds of papers have extended the PH model in myriad directions but little attention has been given to comparing PH to other competing semiparametric specifications. All the four real data analyses in Section 3 show that either the PO or AFT model provides gross improvements in model fit over PH. A second, important result of this work from a practical standpoint is that clever data augmentation schemes can grossly underperform simple, easily computed block-adaptive Metropolis-Hastings samplers applied directly to the posterior density. With judicious choice of blocking and careful use of existing parametric survival model fits, the block-adaptive approach cultivated here is robust, requires no tuning, is relatively fast, and has been applied to data sets of up to a million observations. Furthermore, all of the machinery developed is available in a powerful, freely-available R function `survregbayes` calling compiled C++ in the `spBayesSurv` package (Zhou and Hanson, 2016) for R. Note that although the methodology is developed for both areal and georeferenced spatial time-to-event data, non-spatial data are also accommodated.

Model formulation consists of a parametric portion giving relative risk (PH), odds (PO), or acceleration factors (AFT) coupled with georeferenced or areal spatial frailties, and a nonparametric baseline survival function modeled as a transformed Bernstein polynomial (TBP) (Chen et al., 2014) centered at a standard parametric family: one of log-logistic, log-normal, or Weibull. Centering the baseline allows prior mass to be roughly guided by

the parametric family. The resulting distribution behaves similarly to a B-spline but where knot locations are guided by the centering family, blending the merits of both parametric and nonparametric approaches. Unlike mixtures of Dirichlet processes (Antoniak, 1974), gamma processes (Kalbfleisch, 1978), and mixtures of Polya trees (Lavine, 1992), the TBP is smooth, allowing for efficient block-updating. All manner of observed exactly, right censored, interval censored, and left-truncated data are accommodated, as well as mixtures of these. The Markov chain Monte Carlo (MCMC) scheme does not rely on data augmentation, e.g. imputing censored survival times, and is fully automated. Left-truncation allows for the inclusion of time-dependent covariates and spike-and-slab variable selection is also implemented. Finally, a separate function that computes a variation on the Cox-Snell residual plot allows for gross assessment of model fit.

There is a burgeoning literature on fitting PO and PH models to interval censored data using what is essentially an integrated B-spline, termed a monotone spline, for the baseline cumulative hazard function. Cai et al. (2011) consider a PH model for current status data; Lin and Wang (2011) consider the PO model with current status data; case 2 interval censoring is considered for PO by Wang and Lin (2011). Pan et al. (2014) consider the PH model for general interval censored data with spatial CAR frailties and Lin et al. (2015) consider the same PH model with general interval censored data without frailties. Wang et al. (2016) take the E-M approach to the model of Lin et al. (2015). All of these methods use data augmentation requiring several latent Poisson variables *per subject* to obtain inference. More importantly, these methods *cannot be used with standard right censored data*: the use of data augmentation requires data be fully interval censored, i.e. no survival times can be seen exactly. The TBP prior used here naturally scales with the data; our methods include all of the semiparametric models in the seven papers referenced above as a special case and in addition allow for standard right censored data, left-truncated data, time-dependent covariates, georeferenced spatial frailties as well as areal frailties, variable selection, and easy fitting of the AFT model. The monotone spline prior cannot be easily

used with AFT or scale-based models (such as accelerated hazards and extended hazards) as the density is shrunk or stretched according to acceleration factors and the monotone spline has fixed knots.

Section 2 describes the models including the TBP, georeferenced and areal frailties, MCMC, diagnostics and model selection criteria, a test for parametric baseline, variable selection, left-truncation and time-dependent covariates, and partially linear predictors. Four comprehensive data analyses comprise the bulk of Section 3, including reanalyses of large, complex data sets appearing in other papers analyzed only by PH; the PH model is outperformed by PO or AFT in all four analyses. Section 4 offers extensive simulations illustrating estimation and variable selection, as well as comparing to the R packages `ICBayes` (Pan et al., 2015), `bayesSurv` (Komárek and Lesaffre, 2008) and `R2BayesX` (Umlauf et al., 2015; Belitz et al., 2015). The paper is concluded in Section 5.

2 The Model

Subjects are observed at m distinct spatial locations $\mathbf{s}_1, \dots, \mathbf{s}_m$. For areally-observed outcomes, e.g. county-level, there is typically replication; for georeferenced there may or may not be replication. Let t_{ij} be the (possibly censored) survival time for subject j at location \mathbf{s}_i and \mathbf{x}_{ij} be the corresponding p -dimensional vector of covariates, $i = 1, \dots, m, j = 1, \dots, n_i$. Then $n = \sum_{i=1}^m n_i$ is the total number of subjects. Assume the survival time t_{ij} lies in the interval (a_{ij}, b_{ij}) , $0 \leq a_{ij} \leq b_{ij} \leq \infty$. Here left censored data are of the form $(0, b_{ij})$, right censored (a_{ij}, ∞) , interval censored (a_{ij}, b_{ij}) and uncensored values simply have $a_{ij} = b_{ij}$, i.e., we define $(x, x) = \{x\}$. Note that both current status data and case 2 interval censored data arise as particular special cases.

In many applications spatial dependence often arises among survival outcomes due to region-specific similarities in ecological and/or social environments that are typically not measurable or omitted due to confidentiality concerns. To incorporate such spatial depen-

dence, a traditional way is to introduce random effects (frailties) v_1, \dots, v_m into the linear predictor of survival models. In this paper we consider three commonly-used semiparametric spatial frailty models: AFT, PH, and PO. Given spatially-varying frailties v_1, \dots, v_m , regression effects $\boldsymbol{\beta} = (\beta_1, \dots, \beta_p)'$, and baseline survival $S_0(\cdot)$ with density $f_0(\cdot)$ corresponding to $\mathbf{x}_{ij} = \mathbf{0}$ and $v_i = 0$, the AFT model has survival and density functions

$$S_{\mathbf{x}_{ij}}(t) = S_0(e^{\mathbf{x}'_{ij}\boldsymbol{\beta} + v_i}t), \quad f_{\mathbf{x}_{ij}}(t) = e^{\mathbf{x}'_{ij}\boldsymbol{\beta} + v_i} f_0(e^{\mathbf{x}'_{ij}\boldsymbol{\beta} + v_i}t), \quad (2.1)$$

while the PH model has survival and density

$$S_{\mathbf{x}_{ij}}(t) = S_0(t)^{e^{\mathbf{x}'_{ij}\boldsymbol{\beta} + v_i}}, \quad f_{\mathbf{x}_{ij}}(t) = e^{\mathbf{x}'_{ij}\boldsymbol{\beta} + v_i} S_0(t)^{e^{\mathbf{x}'_{ij}\boldsymbol{\beta} + v_i} - 1} f_0(t), \quad (2.2)$$

and the PO model has survival and density

$$S_{\mathbf{x}_{ij}}(t) = \frac{e^{-\mathbf{x}'_{ij}\boldsymbol{\beta} - v_i} S_0(t)}{1 + (e^{-\mathbf{x}'_{ij}\boldsymbol{\beta} - v_i} - 1) S_0(t)}, \quad f_{\mathbf{x}_{ij}}(t) = \frac{e^{-\mathbf{x}'_{ij}\boldsymbol{\beta} - v_i} f_0(t)}{[1 + (e^{-\mathbf{x}'_{ij}\boldsymbol{\beta} - v_i} - 1) S_0(t)]^2}. \quad (2.3)$$

In semiparametric survival analysis, a wide variety of Bayesian nonparametric priors can be used to model S_0 ; see Müller et al. (2015) and Zhou and Hanson (2015) for reviews. In this paper we consider the models (2.1), (2.2) and (2.3) with a transformed Bernstein polynomial (TBP) prior (Chen et al., 2014) on S_0 . The TBP prior is attractive in that it is centered at a given parametric family and it selects smooth densities.

2.1 Transformed Bernstein Polynomial Prior

For a given positive integer J , define a mixture of Bernstein polynomials by

$$b(x|J, \mathbf{w}_J) = \sum_{j=1}^J w_j \beta(x|j, J - j + 1), \quad (2.4)$$

where $\mathbf{w}_J = (w_1, \dots, w_J)'$ is a vector of positive weights satisfying $\sum_{j=1}^J \mathbf{w}_j = 1$ and $\beta(\cdot|a, b)$ denotes a beta density with parameters (a, b) . Clearly $b(x|J, \mathbf{w}_J)$ is a density function and is very flexible, so that, in fact, any density with support $(0, 1)$ can be well approximated using a mixture of only a relatively few beta densities: if $f(x)$ is any continuously differentiable density with support $(0, 1)$ and bounded second derivative, \mathbf{w}_J can be chosen such that

$$\sup_{0 < x < 1} |f(x) - b(x|J, \mathbf{w}_J)| = O(J^{-1}).$$

Integrating (2.4) gives the corresponding cumulative distribution function (cdf)

$$B(x|J, \mathbf{w}_J) = \sum_{j=1}^J w_j I_x(j, J - j + 1), \quad (2.5)$$

where $I_x(a, b)$ is the cdf associated with $\beta(x|a, b)$. One can calculate (2.5) recursively as

$$I_x(j+1, J-j) = I_x(j, J-j+1) - \frac{\Gamma(J+1)}{\Gamma(j+1)\Gamma(J-j+1)} x^j (1-x)^{J-j}.$$

By assigning a joint prior distribution to (J, \mathbf{w}_J) , the random $b(x|J, \mathbf{w}_J)$ in (2.4) is said to have the Bernstein polynomial (BP) prior. Petrone (1999) showed that if the prior on (J, \mathbf{w}_J) has full support, the BP prior has positive support on all continuous density functions on $(0, 1)$. However, for practical reasons, the degree J is often truncated to a large value, say K , so that the prior has support $\mathcal{B}_K = \{b(x|J, \mathbf{w}_J) : J \leq K\}$. Under mild conditions, Petrone and Wasserman (2002) showed that, for a fixed K , the posterior density almost surely converges to a density that minimizes the Kullback-Leibler divergence of the true density against $b(x) \in \mathcal{B}_K$. We fix $J \equiv K = 15$ throughout by noting that BP priors of lesser degree have the same support as \mathcal{B}_K because any Bernstein polynomial can be written in terms of Bernstein polynomials of higher degree through

$$\beta_{j, J-1}(x) = \frac{J-j}{J} \beta_{j, J}(x) + \frac{j}{J} \beta_{j+1, J}(x),$$

where $\beta_{j,J}(x) = \beta(x|j, J-j+1)$. It follows that $b(x|J-1, \mathbf{w}_{J-1})$ can be written as $b(x|J, \mathbf{w}_J^*)$ with suitable choice of \mathbf{w}_J^* , so every $b(x|J, \mathbf{w}_J)$ with $J \leq K$ belongs to $\{b(x|K, \mathbf{w}_K)\}$. Regarding the prior for \mathbf{w}_J , we consider a Dirichlet distribution, $\mathbf{w}_J|J \sim \text{Dirichlet}(\alpha, \dots, \alpha)$, where $\alpha > 0$ is a precision parameter. An attractive property of the BP prior specified above is that $E[b(x|J, \mathbf{w}_J)] = \sum_{j=1}^J \beta(x|j, J-j+1)/J = 1$ and $E[B(x|J, \mathbf{w}_J)] = x$ for $x \in (0, 1)$.

We next describe how to define a random survival function S_0 based on (2.4). Let $\{S_{\boldsymbol{\theta}} : \boldsymbol{\theta} \in \boldsymbol{\Theta}\}$ denote a parametric family of survival functions with support on positive reals \mathbb{R}^+ . A log-logistic family $S_{\boldsymbol{\theta}}(t) = \{1 + (e^{\theta_1}t)^{\exp(\theta_2)}\}^{-1}$ is considered throughout due to its stability and closed form for the survival function and density, where $\boldsymbol{\theta} = (\theta_1, \theta_2)'$. In our experience, Weibull and log-normal baseline distributions yield almost identical posterior inference. Note that $S_{\boldsymbol{\theta}}(t)$ always lies in the interval $(0, 1)$ for $0 < t < \infty$, so a natural prior on S_0 , termed the transformed Bernstein polynomial (TBP) prior, can be defined as

$$S_0(t) = B(S_{\boldsymbol{\theta}}(t)|J, \mathbf{w}_J) \text{ with density } f_0(t) = b(S_{\boldsymbol{\theta}}(t)|J, \mathbf{w}_J)f_{\boldsymbol{\theta}}(t), \quad (2.6)$$

where $f_{\boldsymbol{\theta}}$ is the density associated with $S_{\boldsymbol{\theta}}$. Clearly, the random distribution S_0 is centered at $S_{\boldsymbol{\theta}}$, that is, $E[S_0(t)] = S_{\boldsymbol{\theta}}(t)$ and $E[f_0(t)] = f_{\boldsymbol{\theta}}(t)$. The weight parameters \mathbf{w}_J “adjust” the shape of the baseline survival S_0 relative to the prior guess $S_{\boldsymbol{\theta}}$. This adaptability makes the TBP prior attractive in its flexibility, but also anchors the random S_0 firmly about $S_{\boldsymbol{\theta}}$: $w_j = 1/J$ for $j = 1, \dots, J$ implies $S_0(t) = S_{\boldsymbol{\theta}}(t)$ for $t \geq 0$. Moreover, unlike the mixture of Polya trees (Lavine, 1992) or mixture of Dirichlet process (Antoniak, 1974) priors, the TBP prior selects smooth densities, leading to efficient posterior sampling.

The TBP parameter α acts like the precision in a Dirichlet process (Ferguson, 1973), controlling how stochastically “pliable” S_0 is relative to $S_{\boldsymbol{\theta}}$. Large values of α indicate a strong belief that S_0 is close to $S_{\boldsymbol{\theta}}$; as $\alpha \rightarrow \infty$, $S_0 \rightarrow S_{\boldsymbol{\theta}}$ with probability 1. Smaller values of α allow more pronounced deviations of S_0 from $S_{\boldsymbol{\theta}}$. A gamma prior on α is considered: $\alpha \sim \Gamma(a_0, b_0)$ where $E(\alpha) = a_0/b_0$.

2.2 Spatial Frailty Modeling

Spatial frailty models are usually grouped into two general settings according to their underlying data structure (Banerjee et al., 2014): *georeferenced* data, where \mathbf{s}_i varies continuously throughout a fixed study region \mathcal{S} (e.g., \mathbf{s}_i is recorded as longitude and latitude); and *areal* data, where \mathcal{S} is partitioned into a finite number of areal units with well-defined boundaries (e.g., \mathbf{s}_i represents a county).

2.2.1 Areal Data Modeling

We consider an intrinsic conditionally autoregressive (ICAR) prior (Besag, 1974) on $\mathbf{v} = (v_1, \dots, v_m)'$. Let e_{ij} be 1 if regions i and j share a common boundary and 0 otherwise; set $e_{ii} = 0$. Then the $m \times m$ matrix $\mathbf{E} = [e_{ij}]$ is called the adjacency matrix for the m regions. The ICAR prior on \mathbf{v} is defined through the set of the conditional distributions

$$v_i | \{v_j\}_{j \neq i} \sim N \left(\sum_{j=1}^m e_{ij} v_j / e_{i+}, \tau^2 / e_{i+} \right), \quad i = 1, \dots, m, \quad (2.7)$$

where $e_{i+} = \sum_{j=1}^m e_{ij}$ and τ^2 / e_{j+} . The induced prior on \mathbf{v} under ICAR is improper; the constraint $\sum_{j=1}^m v_j = 0$ is used for identifiability (Banerjee et al., 2014).

2.2.2 Georeferenced Data Modeling

For georeferenced data, it is commonly assumed that $v_i = v(\mathbf{s}_i)$ arises from a Gaussian random field (GRF) $\{v(\mathbf{s}), \mathbf{s} \in \mathcal{S}\}$ such that $\mathbf{v} = (v_1, \dots, v_m)$ follows a multivariate Gaussian distribution as $\mathbf{v} \sim N_m(\mathbf{0}, \tau^2 \mathbf{R})$, where τ^2 measures the amount of spatial variation across locations and the (i, j) element of \mathbf{R} is modeled as $\mathbf{R}[i, j] = \rho(d_{ij})$. Here $\rho(\cdot)$ is a correlation function controlling the spatial dependence of $v(\mathbf{s})$, and d_{ij} is the distance (e.g., Euclidean, great-circle) between \mathbf{s}_i and \mathbf{s}_j . In this paper, we consider the powered exponential correlation function $\rho(d_{ij}; \phi) = \exp\{-(\phi d_{ij})^\nu\}$, where $\phi > 0$ controls the spatial decay over distance,

and $\nu \in (0, 2]$ is a shape parameter. Similar to ICAR, the conditional prior is given by

$$v_i | \{v_j\}_{j \neq i} \sim N \left(- \sum_{\{j: j \neq i\}} p_{ij} v_j / p_{ii}, \tau^2 / p_{ii} \right), \quad i = 1, \dots, m, \quad (2.8)$$

where p_{ij} is the (i, j) element of \mathbf{R}^{-1} .

As m increases evaluating \mathbf{R}^{-1} from \mathbf{R} becomes computationally impractical. Various approaches have been developed to overcome this computational issue such as process convolutions (Higdon, 2002), fixed rank kriging (Cressie and Johannesson, 2008), predictive process models (Banerjee et al., 2008), sparse approximations (Kaufman et al., 2008), and the full-scale approximation (Sang and Huang, 2012). We consider the full-scale approximation (FSA) here due to its capability of capturing both large- and small-scale spatial dependence; see supplementary Appendix B for a brief introduction.

The FSA was arrived at after a number of lengthy, unsuccessful attempts at using other approximations. BayesX (Belitz et al., 2015) uses what have been termed “Matern splines,” first introduced in an applied context by Kammann and Wand (2003). Several authors have used this approach including Kneib (2006), Hennerfeind et al. (2006), and Kneib and Fahrmeir (2007). This approximation was termed a “predictive process” and given a more formal treatment by Banerjee et al. (2008). In our experience, the predictive process tends to give biased regression effects and prediction when the rank (i.e. the number of knots) was chosen too low; the problem worsened with no replication and/or when spatial correlation was high. The FSA fixes the predictive process by adding tapering to the “residual” process. We have been able to successfully analyze data with several thousand georeferenced spatial locations via MCMC using the FSA with little to no artificial bias in parameter estimation and consistently good predictive ability.

2.3 Likelihood Construction and MCMC

Let $\mathcal{D} = \{(a_{ij}, b_{ij}, \mathbf{x}_{ij}, \mathbf{s}_i); i = 1, \dots, m, j = 1, \dots, n_i\}$ be the observed data. Assume $t_{ij}|v_i \sim S_{\mathbf{x}_{ij}}(t)$ following one of (2.1), (2.2), or (2.3) with the TBP prior on $S_0(t)$ defined in (2.6), and \mathbf{v} following (2.7) or (2.8). The likelihood for $(\mathbf{w}_J, \boldsymbol{\theta}, \boldsymbol{\beta}, \mathbf{v})$ is

$$L(\mathbf{w}_J, \boldsymbol{\theta}, \boldsymbol{\beta}, \mathbf{v}) = \prod_{i=1}^m \prod_{j=1}^{n_i} [S_{\mathbf{x}_{ij}}(a_{ij}) - S_{\mathbf{x}_{ij}}(b_{ij})]^{I\{a_{ij} < b_{ij}\}} f_{\mathbf{x}_{ij}}(a_{ij})^{I\{a_{ij} = b_{ij}\}}. \quad (2.9)$$

MCMC is carried out through an empirical Bayes approach coupled with adaptive Metropolis samplers (Haario et al., 2001). The posterior density is

$$p(\mathbf{w}_J, \boldsymbol{\theta}, \boldsymbol{\beta}, \mathbf{v}, \alpha, \tau^2, \phi | \mathcal{D}) \propto L(\mathbf{w}_J, \boldsymbol{\theta}, \boldsymbol{\beta}, \mathbf{v}) p(\mathbf{w}_J | \alpha) p(\alpha) p(\boldsymbol{\theta}) p(\boldsymbol{\beta}) p(\mathbf{v} | \tau^2) p(\tau^2) p(\phi),$$

where each $p(\cdot)$ represents a prior density, and $p(\phi)$ is only included for georeferenced data. Assume $\boldsymbol{\theta} \sim N_2(\boldsymbol{\theta}_0, \mathbf{V}_0)$, $\boldsymbol{\beta} \sim N_p(\boldsymbol{\beta}_0, \mathbf{S}_0)$, $\alpha \sim \Gamma(a_0, b_0)$, $\tau^{-2} \sim \Gamma(a_\tau, b_\tau)$ and $\phi \sim \Gamma(a_\phi, b_\phi)$.

Recall that $w_j = 1/J$ implies the underlying parametric model with $S_0(t) = S_{\boldsymbol{\theta}}(t)$. Thus, the parametric model provides good starting values for the TBP survival model. Let $\hat{\boldsymbol{\theta}}$ and $\hat{\boldsymbol{\beta}}$ denote the parametric MLEs of $\boldsymbol{\theta}$ and $\boldsymbol{\beta}$, and let $\hat{\mathbf{V}}$ and $\hat{\mathbf{S}}$ denote their estimated covariance matrices, respectively. Set $\mathbf{z}_{J-1} = (z_1, \dots, z_{J-1})'$ with $z_j = \log(w_j) - \log(w_J)$. The $\boldsymbol{\beta}$, $\boldsymbol{\theta}$, \mathbf{z}_{J-1} , α and ϕ are all updated using adaptive Metropolis samplers, where the initial proposal variance is $\hat{\mathbf{S}}$ for $\boldsymbol{\beta}$, $\hat{\mathbf{V}}$ for $\boldsymbol{\theta}$, $0.16\mathbf{I}_{J-1}$ for \mathbf{z}_{J-1} and 0.16 for α and ϕ . Each frailty term v_i is updated via Metropolis-Hastings, with proposal variance as the conditional prior variance of $v_i | \{v_j\}_{j \neq i}$; τ^{-2} is updated via a Gibbs step from its full conditional. A complete description and derivation of the updating steps are in supplementary Appendix A.

Regarding the default choice for the hyperparameters, when variable selection is not implemented (see Section 2.6) we set $\boldsymbol{\beta}_0 = \mathbf{0}$, $\mathbf{S}_0 = 10^{10}\mathbf{I}_p$, $\boldsymbol{\theta}_0 = \hat{\boldsymbol{\theta}}$, $\mathbf{V}_0 = 10\hat{\mathbf{V}}$, $a_0 = b_0 = 1$, and $a_\tau = b_\tau = .001$. For georeferenced data, we set $a_\phi = 1$ and choose b_ϕ so that $\Pr(\phi > \phi_0) = 0.95$, where ϕ_0 satisfies $\rho(\max_{i,j} \|\mathbf{s}_i - \mathbf{s}_j\|; \phi_0) = 0.001$. Note here we assume a

somewhat informative prior on $\boldsymbol{\theta}$ to obviate confounding between $\boldsymbol{\theta}$ and \mathbf{w}_J .

2.4 Model Diagnostics and Comparison

For model diagnostics, a general residual defined in Cox and Snell (1968) has been widely used in a variety of regression settings. In the current Bayesian setup, we define the residual as $r(t_{ij}) = -\log\{S_{\mathbf{x}_{ij}}(t_{ij})|\mathcal{D}\}$, where the residual depends on the posterior $[\boldsymbol{\beta}, \boldsymbol{\theta}, \mathbf{w}_J, v_i|\mathcal{D}]$. Given $S_{\mathbf{x}_{ij}}(\cdot)$, $-\log S_{\mathbf{x}_{ij}}(t_{ij})$ has a standard exponential distribution. Therefore, if the model is “correct,” and under the arbitrary censoring, the pairs $\{r(a_{ij}), r(b_{ij})\}$ are approximately a random arbitrarily censored sample from an $\text{Exp}(1)$ distribution, and the estimated (Turnbull, 1974) integrated hazard plot should be approximately straight with slope 1. Uncertainty in the plot is assessed through several cumulative hazards based on a random sample from $[\boldsymbol{\beta}, \boldsymbol{\theta}, \mathbf{w}_J, v_i|\mathcal{D}]$. This is in contrast to typical Cox-Snell plots which only use point estimates.

Several researchers have pointed out that Cox-Snell residuals are conservative in that they may be straight even under quite large departures from the model (Baltazar-Aban and Pena, 1995; O’Quigley and Xu, 2005). In this case, model criteria will be more informative. We consider two popular model choice criteria: the deviance information criterion (DIC) (Spiegelhalter et al., 2002) and the log pseudo marginal likelihood (LPML) (Geisser and Eddy, 1979), where the former places emphasis on the relative quality of model fitting and the latter focuses on the predictive performance. Both criteria are readily computed from the MCMC output; see supplemental Appendix C for more details.

2.5 Parametric vs. Nonparametric S_0

Many authors have found parametric models to fit as well or better than competing semi-parametric models (Cox and Oakes, 1984, p. 123; Nardi and Schemper, 2003). Here, testing for the adequacy of the simpler underlying parametric model is developed. The semiparametric TBP models have their baseline survival functions centered at a parametric family $S_{\boldsymbol{\theta}}(t)$. Note that $\mathbf{z}_{J-1} = \mathbf{0}$ implies $S_0(t) = S_{\boldsymbol{\theta}}(t)$. Therefore, testing $H_0 : \mathbf{z}_{J-1} = \mathbf{0}$ versus

$H_1 : \mathbf{z}_{J-1} \neq \mathbf{0}$ leads to the comparison of the semiparametric model with the underlying parametric model. Let BF_{10} be the Bayes factor between H_1 and H_0 . Zhou et al. (2016) proposed to estimate BF_{10} by a large-sample approximation to the generalized Savage-Dickey density ratio (Verdinelli and Wasserman, 1995). Adapting their approach BF_{10} is estimated

$$\widehat{BF}_{10} = \frac{p(\mathbf{0}|\hat{\alpha})}{N_{J-1}(\mathbf{0}; \hat{\mathbf{m}}, \hat{\Sigma})}, \quad (2.10)$$

where $p(\mathbf{0}|\alpha) = \Gamma(\alpha J)/[J^\alpha \Gamma(\alpha)]^J$ is the prior density of \mathbf{z}_{J-1} evaluated at $\mathbf{z}_{J-1} = \mathbf{0}$, $\hat{\alpha}$ is the posterior mean of α , $N_p(\cdot; \mathbf{m}, \Sigma)$ denotes a p -variable normal density with mean \mathbf{m} and covariance Σ , and $\hat{\mathbf{m}}$ and $\hat{\Sigma}$ are posterior mean and covariance of \mathbf{z}_{J-1} .

2.6 Variable Selection

There is a large amount of literature on Bayesian variable selection methods; see O'Hara et al. (2009) for a comprehensive review. The most direct approach is to multiply β_k by a latent Bernoulli variable γ_k , where $\gamma_k = 1$ indicates presence of covariate x_k in the model, and then assume an appropriate prior on $(\boldsymbol{\beta}, \boldsymbol{\gamma})$, where $\boldsymbol{\gamma} = (\gamma_1, \dots, \gamma_p)$. Kuo and Mallick (1998) considered an independent prior $p(\boldsymbol{\beta}, \boldsymbol{\gamma}) = N_p(\mathbf{0}, \mathbf{S}_0) \times \prod_{k=1}^p \text{Bern}(q_k)$, where \mathbf{S}_0 was taken as a diagonal matrix yielding a diffuse prior on $\boldsymbol{\beta}$, and q_k is a prior probability of including x_k in the model. The resulting MCMC algorithm does not require any tuning, but mixing can be poor if the prior on $\boldsymbol{\beta}$ is too diffuse (O'Hara et al., 2009). The g -prior of Zellner (1983) and its various extensions (Bové et al., 2011; Hanson et al., 2014) have been widely used for variable selection. We consider one such prior adapted for use in the semiparametric survival models considered here. Specifically, the same independent prior as Kuo and Mallick (1998) is considered, but with

$$\boldsymbol{\beta} \sim N_p(\mathbf{0}, gn(\mathbf{X}'\mathbf{X})^{-1}), \quad (2.11)$$

where \mathbf{X} is the usual design matrix, but with mean-centered covariates, i.e. $\mathbf{1}'_n \mathbf{X} = \mathbf{0}'_p$. Assume the covariate vectors \mathbf{x}_{ij} arise from the distribution $\mathbf{x} \sim H(d\mathbf{x})$, independent of $\boldsymbol{\beta}$. Following Hanson et al. (2014) g is set equal to a constant based on prior information on $e^{\mathbf{x}'\boldsymbol{\beta}}$, i.e. the relative risks (PH), acceleration factors (AFT), or odds factors (PO) of random subjects \mathbf{x} relative to their mean $\int_{\mathcal{X}} \mathbf{x} H(d\mathbf{x})$. Under the prior (2.11), Hanson et al. (2014) showed that $\mathbf{x}'\boldsymbol{\beta}$ has an approximately normal distribution with mean 0 and variance ng . Thus, a simple method of choosing g is to pick a number M such that a random $e^{\mathbf{x}'\boldsymbol{\beta}}$ is less than M with probability q . It follows that $g = [\log M / \Phi^{-1}(q)]^2 / p$. Here, $M = 10$ and $q = 0.9$ are fixed. The MCMC procedure is described in supplementary Appendix A.

2.7 Left-Truncation and Time-Dependent Covariates

The survival time t_{ij} is left-truncated at $u_{ij} \geq 0$ when u_{ij} is the time when the ij th subject is first observed. Left-truncation often occurs when age is used as the time scale. Given the observed left-truncated data $\mathcal{D} = \{(u_{ij}, a_{ij}, b_{ij}, \mathbf{x}_{ij}, \mathbf{s}_i)\}$, the likelihood function (2.9) becomes

$$L(\mathbf{w}_J, \boldsymbol{\theta}, \boldsymbol{\beta}, \mathbf{v}) = \prod_{i=1}^m \prod_{j=1}^{n_i} [S_{\mathbf{x}_{ij}}(a_{ij}) - S_{\mathbf{x}_{ij}}(b_{ij})]^{I\{a_{ij} < b_{ij}\}} f_{\mathbf{x}_{ij}}(a_{ij})^{I\{a_{ij} = b_{ij}\}} / S_{\mathbf{x}_{ij}}(u_{ij}).$$

Allowing for left-truncation allows the semiparametric AFT, PH and PO models to be easily extended to handle time-dependent covariates. Following Kneib (2006) and Hanson et al. (2009), assume the covariate vector $\mathbf{x}_{ij}(t)$ is a step function that changes at o_{ij} ordered times $t_{ij,1} < \dots < t_{ij,o_{ij}} \leq a_{ij}$, i.e.,

$$\mathbf{x}_{ij}(t) = \sum_{k=1}^{o_{ij}} \mathbf{x}_{ij,k} I(t_{ij,k} \leq t < t_{ij,k+1}),$$

where $t_{ij,1} = u_{ij}$ and $t_{ij,o_{ij}+1} = \infty$. Assuming one of PH, PO, or AFT holds conditionally on each interval, the survival function for the ij th individual at time a_{ij} is

$$\begin{aligned} P(t_{ij} > a_{ij}) &= P(t_{ij} > a_{ij} | t_{ij} > t_{ij,o_{ij}}) \prod_{k=1}^{o_{ij}} P(t_{ij} > t_{ij,k} | t_{ij} > t_{ij,k-1}) \\ &= \frac{S_{\mathbf{x}_{ij,o_{ij}}}(a_{ij})}{S_{\mathbf{x}_{ij,o_{ij}}}(t_{ij,o_{ij}})} \prod_{k=1}^{o_{ij}} \frac{S_{\mathbf{x}_{ij,k}}(t_{ij,k})}{S_{\mathbf{x}_{ij,k}}(t_{ij,k-1})}, \end{aligned}$$

where $t_{ij,0} = 0$. This leads to the usual PH model for time-dependent covariates (Cox, 1972), the AFT model first proposed by Prentice and Kalbfleisch (1979) and developed by Hanson et al. (2009), and particular piecewise PO model. Thus one can replace the observation $(u_{ij}, a_{ij}, b_{ij}, \mathbf{x}_{ij}(t), \mathbf{s}_i)$ by a set of new o_{ij} observations $(t_{ij,1}, t_{ij,2}, \infty, \mathbf{x}_{ij,1}, \mathbf{s}_i)$, $(t_{ij,2}, t_{ij,3}, \infty, \mathbf{x}_{ij,2}, \mathbf{s}_i)$, \dots , $(t_{ij,o_{ij}}, a_{ij}, b_{ij}, \mathbf{x}_{ij,o_{ij}}, \mathbf{s}_i)$. This way we get a new left-truncated data set of size $N = \sum_{i=1}^m \sum_{j=1}^{n_i} o_{ij}$. Then the likelihood function becomes

$$\begin{aligned} L(\mathbf{w}_J, \boldsymbol{\theta}, \boldsymbol{\beta}, \mathbf{v}) &= \prod_{i=1}^m \prod_{j=1}^{n_i} \left\{ \left[S_{\mathbf{x}_{ij,o_{ij}}}(a_{ij}) - S_{\mathbf{x}_{ij,o_{ij}}}(b_{ij}) \right]^{I\{a_{ij} < b_{ij}\}} f_{\mathbf{x}_{ij,o_{ij}}}(a_{ij})^{I\{a_{ij} = b_{ij}\}} \right. \\ &\quad \left. \times \prod_{k=1}^{o_{ij}} \frac{S_{\mathbf{x}_{ij,k}}(t_{ij,k})}{S_{\mathbf{x}_{ij,k}}(t_{ij,k-1})} \right\}. \end{aligned}$$

2.8 Partially linear predictors

An additive PH model was first considered by Gray (1992) as

$$h_{\mathbf{x}_{ij}}(t) = h_0(t) \exp\{\mathbf{x}'_{ij}\boldsymbol{\beta} + \sum_{\ell=1}^p b_{\ell}(x_{ij\ell})\},$$

where the nonlinear functions $b_1(\cdot), \dots, b_p(\cdot)$ are modeled via penalized B-splines with the linear portion removed. Setting some of the $b_{\ell}(\cdot) \equiv 0$ gives the so-called “partially linear PH model” that has been given a great deal of attention in recent literature. This model has been extended to spatial versions by Kneib (2006) and Hennenfeind et al. (2006) for PH and can be easily fit in `R2BayesX`. Additive partially linear predictors can be implemented

in the proposed AFT, PH and PO models by simply adding a linear basis expansion for any continuous covariate; these include harmonic expansions, wavelets, various polynomials including fractional polynomials, and splines. Of all of these, we have had the best overall luck with B-splines. Specifically, the $b_\ell(\cdot)$ is parameterized as

$$b_\ell(\cdot) = \sum_{k=1}^K \xi_{\ell k} B_{\ell k}(\cdot),$$

where $\{B_{\ell k}(\cdot) : k = 0, \dots, K+1\}$ are the standard cubic B-spline basis functions with knots determined by the data; the first and last basis functions have been dropped to ensure a full-rank model (the linear term is already included). Independent normal priors are considered for $\boldsymbol{\beta}$ and $\boldsymbol{\xi}_\ell = (\xi_{\ell 1}, \dots, \xi_{\ell K})'$:

$$\boldsymbol{\beta} \sim N(\mathbf{0}, \mathbf{S}_0), \quad \boldsymbol{\xi}_\ell \sim N(\mathbf{0}, gn(\mathbf{X}'_\ell \mathbf{X}_\ell)^{-1}), \ell = 1, \dots, p$$

where $\mathbf{S}_0 = 10^{10} \mathbf{I}_p$, \mathbf{X}_ℓ is the design matrix for the $b_\ell(\cdot)$ term, and $g = [\log 10 / \Phi^{-1}(0.9)]^2 / K$. Note posterior updating could be ineffeiciant if a large number of predictors are considered, as $(\boldsymbol{\beta}, \boldsymbol{\xi}_1, \dots, \boldsymbol{\xi}_p)$ is currently updated all at once via adaptive Metropolis.

Bayes factors can be used to test the linearity of $x_{ij\ell}$ through the hypothesis $H_0 : \boldsymbol{\xi}_\ell = \mathbf{0}$ versus $H_1 : \boldsymbol{\xi}_\ell \neq \mathbf{0}$. Let BF_{10} be the Bayes factor between H_1 and H_0 . We estimate BF_{10} by a large-sample approximation to the Savage-Dickey density ratio (Dickey, 1971)

$$\widehat{BF}_{10} = \frac{N_K(\mathbf{0}; \mathbf{0}, gn(\mathbf{X}'_\ell \mathbf{X}_\ell)^{-1})}{N_K(\mathbf{0}; \hat{\mathbf{m}}_\ell, \hat{\boldsymbol{\Sigma}}_\ell)}, \quad (2.12)$$

where $\hat{\mathbf{m}}_\ell$ and $\hat{\boldsymbol{\Sigma}}_\ell$ are posterior mean and covariance of $\boldsymbol{\xi}_\ell$.

3 Real Data Applications

3.1 Childhood Mortality Data in Nigeria

The first analysis uses data from the 2003 Nigeria Demographic and Health Survey (NDHS); see National Population Commission (NPC) [Nigeria] and ORC Macro (2004) for details. The 2003 NDHS interviewed all women in reproductive age 15–49 years from a nationally representative sample of over 7,000 households, and collected the mortality information on a total of 6,029 children who were born within 5 years prior to the survey. We consider age at death of the child. According to the description of the DHS Individual Recode Data File, “...age at death is usually reported in days if it was less than one month, in months if it was less than two years and otherwise in years.” If the child was still alive by the date of interview, the survival time is right censored and the right censoring time can be calculated in days (i.e., from the child’s birth date to the date of interview). Because of this inconsistency of time units, Kneib (2006) recommended the use of an interval censored model instead of a classical right censored model. Thus all survival times recorded in months or years are treated as interval censored: the date of death is determined by adding the survival time in months or in years to the date of birth. Since only birth month is available for children who died before the interview, the left endpoint is defined as the days between the last day of the birth month and first day of the death month and the right endpoint as the days between the first day of birth month and last day of death month. Of the 843 children who died before the interview, there are 52 children who died right after their birth. In this case we set their survival time to be 0.1 days.

Based on previous studies (e.g., Adebayo and Fahrmeir, 2005; Kneib, 2006), we consider the following risk factors associated with childhood mortality: mother’s age at birth, mother’s body mass index (BMI), the duration of breastfeeding in months, preceding birth interval in months, place of delivery (hospital, other), gender of the child (male, female), mother’s education level (at least primary, no education), place of residence (urban, rural). The first

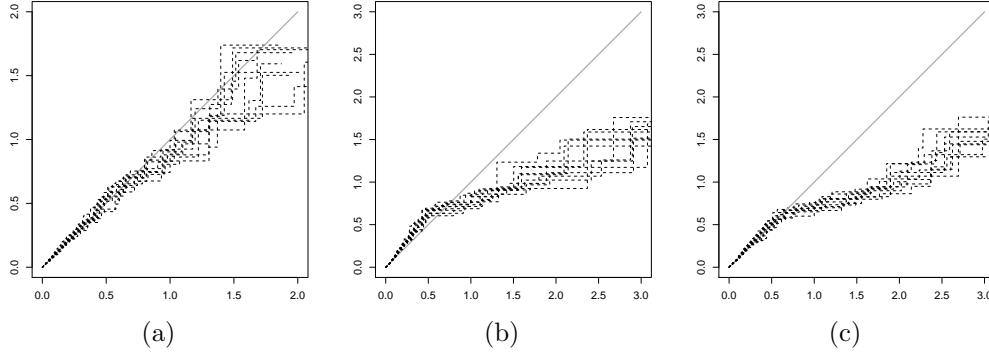


Figure 1: Childhood mortality data. Cox-Snell residual plots under AFT (panel a), PH (panel b) and PO (panel c).

category in each of the above is reference. In addition, one of the $m = 37$ states of residence is available for each child. After removing missing values, the final number of children is given by $n = 4,363$. Supplementary Table S1 reports summary statistics for the data.

We fit the AFT, PH and PO ICAR frailty models with all covariates included, without variable selection. Based upon examination of trace plots for model parameters, for each MCMC we retain 5,000 scans thinned from 50,000 after a burn-in period of 50,000 iterations. The chains mix quite well for all fitted models. Figure 1 presents the Cox-Snell residual plots under each model, where we see that the AFT model fits the data best initially. However, if we note that over 99% of the residuals are less than 0.72 under all three models and focus the plots within that range, we see that the PO and AFT perform equally well and the PH deviates the most. The three models are further compared using the LPML and DIC criteria. Supplementary Table S2 summarizes the results. The PO model significantly outperforms the AFT and PH as measured by both LPML and DIC. Regarding the regression coefficient estimates, we see that mother’s age at birth, mother’s BMI and child’s gender child are all not statistically significant across the three models, and the residence of child is significant under the AFT and PO, but not under the PH.

To choose an optimal set of risk factors, we apply the variable selection algorithm described in Section 2.6; the variable sets with the first three highest frequencies are shown in supplementary Table S3. The covariate set with highest posterior probability under the PO is

Table 1: Childhood mortality data. Posterior means (95% credible intervals) of fixed effects β from fitting the PO ICAR frailty model with selected risk factors.

Breastfeed	-0.357(-0.384, -0.329)
Preceding	-0.015(-0.023, -0.008)
Delivery	-0.504(-0.853, -0.169)
Education	-0.709(-1.021, -0.398)
Residence	-0.330(-0.613, -0.042)
τ^2	0.792(0.264, 1.804)

breastfeeding duration, preceding birth interval, place of delivery, education, and residence; note that the AFT and PH do not select residence in the best covariate set. Considering the PO is the best fitting among the three models in terms of LPML and DIC criteria, we refit the PO model with the selected covariates, as shown in Table 1. The resulting LPML and DIC improve without superfluous variables to -2077 and 4149 from -2079 and 4153 , respectively. All five chosen predictors are significant risk factors for children mortality. For example, higher breastfeeding duration decreases the odds of a child dying by any time; holding other predictors constant, a 2-month increase in duration *cuts the odds of dying in half*, $\exp(-0.357 \times 2) = 0.49$.

The posterior means of spatial frailties for each state are mapped in Figure 2. The map shows that north central states have relatively high frailties, indicating that the childhood mortality rates are expected to be higher in these regions. The three darkest shaded states, from darkest to lightest are Yobe, Jigawa, and Bauchi, largely agricultural areas with relatively limited healthcare and access to potable water.

3.2 Loblolly Pine Survival Data

Loblolly pine is the most commercially important timber species in the Southeastern United States; estimating loblolly survival is crucial to forestry research. The dataset used in this section consists of 45,525 loblolly pine trees at 168 distinct sites, which were established in 1980-1981 and monitored annually until 2001-2002. During the 21-year follow-up, 5,379 trees died; the rest survived until the last follow-up and are treated as right censored. It is

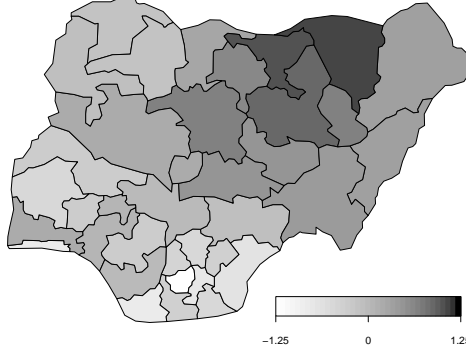


Figure 2: Childhood mortality data. Map for the posterior mean frailties under the PO ICAR frailty model.

of interest to investigate the association between loblolly pine survival and several important risk factors after adjusting for spatial dependence among different sites. The risk factors considered include two time-independent variables, treatment and physiographic region, and three time-dependent variables—diameter at breast height, tree height and crown class—which were repeatedly measured every 3 years. Supplementary Table S4 presents some baseline characteristics for the trees.

Li et al. (2015a) fitted a semiparametric PH model with several georeferenced spatial frailty specifications. However, they showed that the proportional hazard assumption does not hold very well for treatment and physiographic region. To investigate whether the AFT or PO provides better fit, we fit each of the AFT, PH and PO models with GRF frailties to the data using the same covariates as those in Li et al. (2015a). Here we use $\nu = 1$ for the powered exponential correlation function. To better investigate the spatial frailty effect, we also fit each model with independent and identically distributed (IID) Gaussian frailties and non-frailty models. For each MCMC run we retained 2,000 scans thinned from 50,000 after a burn-in period of 10,000 iterations. Figure 3 reports the Cox-Snell residual plots under the three GRF frailty models, where we see that the PH model severely deviates from the 45 degree line, and the AFT fits the data much better than the PH and PO. Table 2 compares all fitted models using the LPML and DIC criteria, where we can see that the AFT always outperforms the PH and PO regardless of the frailty assumptions. Under all three models,

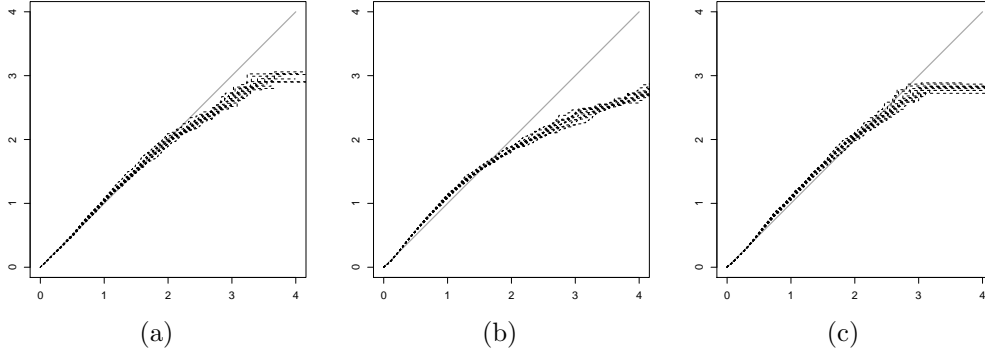


Figure 3: Loblolly pine data. Cox-Snell residual plots under AFT (panel a), PH (panel b) and PO (panel c) with GRF frailties.

Table 2: Loblolly pine data. Model comparison.

		AFT	PH	PO
GRF frailty	LPML	-23,812	-23,991	-23,882
	DIC	47,611	47,971	47,767
IID frailty	LPML	-23,832	-23,966	-23,865
	DIC	47,648	47,897	47,731
Non-frailty	LPML	-25,447	-25,508	-25,549
	DIC	50,893	51,015	51,099

incorporating IID frailties has significantly improved the goodness of fit of the non-frailty model. Some goodness of fit improvement for the GRF over the IID occurs under the AFT, but this does not happen under the PH and PO, indicating that adding spatially structured frailties can deteriorate the model if the overarching model assumption is violated.

Table 3 gives covariate effects under the AFT models. Coefficient estimates under the model with frailties (IID or GRF) have changed significantly from those under the non-frailty model. For example, the effect of total tree height on tree survival is reversed when the model is fit with frailties. This indicates that shorter trees are associated with longer survival rates overall, while in the local scale taller trees have better survival rates than shorter trees adjusting for spatial variation.

We next interpret the results under the AFT for time-dependent covariates model (Pren- tice and Kalbfleisch, 1979) with GRF frailties, as it outperforms all other models. Table 3 shows all covariates are significant risk factors for loblolly pine survival. For example, the

Table 3: Loblolly pine data. Posterior means (95% credible intervals) of fixed effects β from fitting the AFT model with different frailty settings.

	Non-frailty	IID frailty	GRF frailty
DBH	-0.233(-0.255,-0.212)	-0.127(-0.144,-0.111)	-0.126(-0.142,-0.110)
TH	0.027(0.024,0.030)	-0.012(-0.015,-0.010)	-0.011(-0.014,-0.009)
treat2	-0.521(-0.583,-0.466)	-0.381(-0.423,-0.339)	-0.388(-0.431,-0.349)
treat3	-0.719(-0.798,-0.641)	-0.529(-0.589,-0.473)	-0.544(-0.601,-0.495)
PhyReg2	-0.302(-0.367,-0.241)	-0.362(-0.514,-0.198)	-0.390(-0.594,-0.201)
PhyReg3	-0.007(-0.110,0.099)	-0.254(-0.530,0.050)	-0.260(-0.511,0.014)
C2	0.097(0.028,0.169)	0.031(-0.023,0.078)	0.044(-0.002,0.097)
C3	0.835(0.747,0.923)	0.401(0.331,0.465)	0.430(0.375,0.491)
C4	1.919(1.799,2.029)	1.040(0.951,1.128)	1.101(1.018,1.194)
treat2:PhyReg2	0.146(0.041,0.244)	0.118(0.053,0.190)	0.105(0.046,0.168)
treat3:PhyReg2	0.372(0.246,0.503)	0.255(0.169,0.349)	0.246(0.162,0.332)
treat2:PhyReg3	-0.404(-0.625,-0.197)	-0.220(-0.374,-0.072)	-0.216(-0.368,-0.064)
treat3:PhyReg3	0.109(-0.129,0.325)	0.110(-0.067,0.267)	0.125(-0.037,0.286)
τ^2		0.318(0.248,0.402)	0.350(0.270,0.457)
ϕ			0.274(0.165,0.434)

mean or median survival time will increase by a factor $e^{0.126} = 1.134$ for every 1cm increase in diameter at breast height, holding other covariates and the frailty constant. Hanson et al. (2009) note that this interpretation holds for mean or median *residual life* as well, which is of greater interest in medical contexts when choosing a course of treatment. Significant interaction effects are present between treatment and physiographic region; Figure 4 presents the survival curves for the treatment effect under different physiographic regions. The thinning treatment has the largest effect on survival rates in coastal regions, while for piedmont regions, heavy thinning is required to improve survival rates. The posterior means of spatial frailties for each location are also mapped in Figure 4, where we do not see a clear spatial pattern, implying that the spatial dependence may not be very strong for these data. To further confirm this, the posterior mean of the spatial range parameter ϕ is 0.274. Note that 99% of the pairwise distances among the 168 locations are greater than 9.93 km, that is, 99% of the pairwise correlations are lower than $1 - e^{-0.274 \times 9.93} \approx 0.066$.

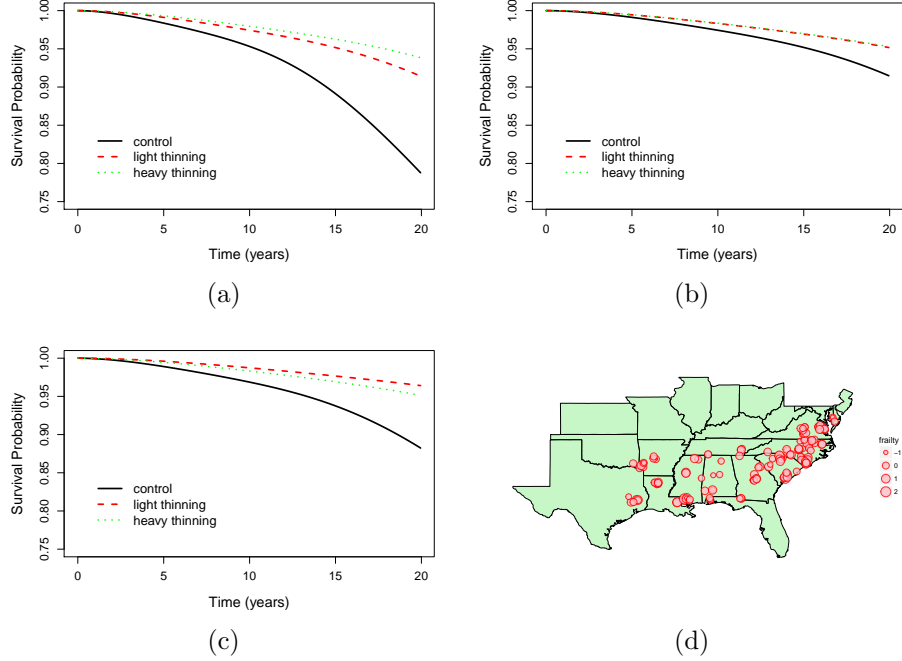


Figure 4: Loblolly pine data. Survival curves for treatment effect under coastal region (panel a), piedmont (panel b) and other region (panel c). The posterior means of spatial frailties for each location are mapped in panel d.

3.3 The Signal Tandmobiel Study

Oral health data collected from the Signal Tandmobiel study are next considered, available in the R package `bayesSurv`; a description of the data set can be found in Komárek and Lesaffre (2009). It is of interest to investigate the impact of gender (1 = girl, 0 = boy), dmf (1, if the predecessor of the permanent first premolar was decayed, missing due to caries or filled, 0, if the predecessor was sound), and tooth location (1 = mandibular, 0 = maxillary) on the emergence time of each of the four permanent first premolar (teeth 14, 24, 34, 44). The data set consists of 4,430 children with four tooth emergence times recorded for each child, yielding a sample size of $n = 17,594$. The emergence times are interval censored due to annual examinations. Komárek and Lesaffre (2009) fit an IID Gaussian frailty AFT model for taking into account the dependency between emergence times within each child. However, it is unknown whether the AFT is the best model compared to the PH and PO. Each of the AFT, PH and PO models with IID frailties were fit to the data using the same

Table 4: The Signal Tandmobiel study. Posterior means (95% credible intervals) of fixed effects from fitting the AFT, PH and PO models with IID frailties. The LPML and DIC are also shown for each model.

	AFT (LPML: -15143) (DIC: 29046)	PH (LPML: -15240) (DIC: 30047)	PO (LPML: -15519) (DIC: 30577)
gender	0.045(0.038, 0.053)	1.026(0.869, 1.193)	1.449(1.225, 1.676)
dmf	0.031(0.027, 0.036)	0.791(0.684, 0.899)	1.419(1.254, 1.585)
tooth	0.020(0.017, 0.022)	0.406(0.339, 0.471)	0.593(0.500, 0.692)
dmf:tooth	-0.018(-0.022, -0.014)	-0.472(-0.575, -0.373)	-0.768(-0.922, -0.618)
gender:dmf	-0.009(-0.015, -0.003)	-0.257(-0.392, -0.127)	-0.464(-0.664, -0.262)
τ^2	0.010(0.009, 0.010)	4.573(4.273, 4.900)	9.348(8.738, 9.978)

covariates as the Model S in (Komárek and Lesaffre, 2009, Table 4) giving LPML values -15143, -15240, and -15519, respectively. Thus, the AFT model significantly outperforms the PH and PO in terms of predictive performance. Table 4 reports the fixed effects and frailty variances under each model, from which we see that the effect of dmf is different for boys and girls, and it is also different for mandibular and maxillary teeth.

3.4 Leukemia Data

Finally, a dataset on the survival of acute myeloid leukemia in $n = 1,043$ patients is considered, available for access in Fahrmeir and Kneib (2011). It is of interest to investigate possible spatial variation in survival after accounting for known subject-specific prognostic factors, which include age, sex, white blood cell count (wbc) at diagnosis, and the Townsend score (tpi) for which higher values indicates less affluent areas. There are 24 administrative districts and each one forms a spatial cluster. Henderson et al. (2002) fitted a multivariate gamma frailty PH model with linear predictors. Here we fit each of the PH, AFT and PO models with ICAR frailties to see whether the AFT or PO model provides better fit. To allow for non-linear effects of continuous predictors, we consider partially linear age, wbc and tpi as described in Section 2.8.

The LPML values for the PH, AFT and PO models are -5946, -5945, and -5919, re-

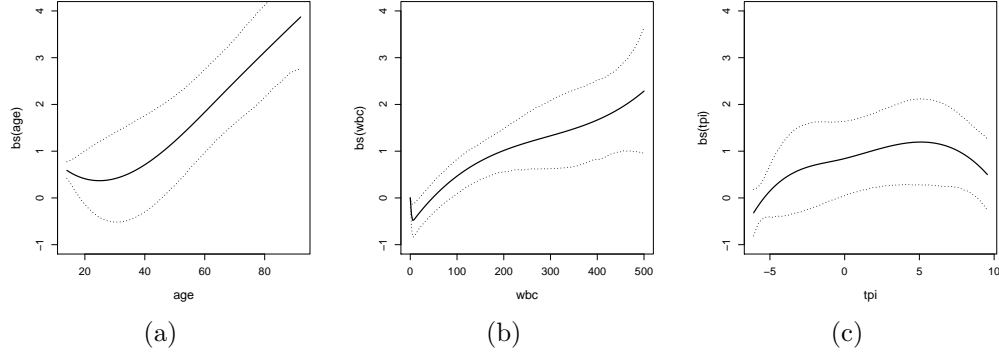


Figure 5: Leukemia data. Posterior mean estimates (solid lines) for the effects of age (panel a), wbc (panel b) and tpi (panel c), together with 95% credible intervals (dotted lines).

spectively. The PO model significantly outperforms others from a predictive point of view. Figure 5 presents the estimated effects of age, wbc and tpi under the PO model, where we do observe some mild nonlinearity. The Bayes Factors for testing the linearity of age, wbc and tpi are 0.13, 0.04 and 0.01, respectively; non-linear effects are not needed.

4 Simulation

Extensive simulations were carried out to evaluate the proposed MCMC algorithms (implemented in `spBayesSurv`) under the three survival models with arbitrarily censored spatial data. We then compare our approach with the data augmentation method (Lin et al., 2015) implemented in `ICBayes`, the Bayesian G-splines method (Komarek, 2006) implemented in `bayesSurv`, and the geoaddivitive PH modeling (Hennerfeind et al., 2006) implemented in `R2BayesX`. Additional simulations for georeferenced data and variable selections are available in supplementary Appendixes F.2 and F.3.

4.1 Simulation I: Areal Data

For each of the AFT, PH and PO, data were generated from (2.1), (2.2) and (2.3), respectively, where $\mathbf{x}_{ij} = (x_{ij1}, x_{ij2})'$ with $x_{ij1} \stackrel{iid}{\sim} \text{Bernoulli}(0.5)$ and $x_{ij2} \stackrel{iid}{\sim} N(0, 1)$, $i = 1 \dots, 37, j = 1, \dots, 20$, $\boldsymbol{\beta} = (\beta_1, \beta_2)' = (1, 1)'$, $S_0(t) = 1 - 0.5[\Phi(2(\log t + 1)) + \Phi(2(\log t - 1))]$,

and v_i follows the ICAR model (2.7) with $\tau^2 = 1$ and \mathbf{E} being the Nigeria adjacency matrix used in the childhood mortality data analysis. The sample size is $n = 740$. To obtain arbitrarily censored data, we applied right censoring scheme to a half of the sample data and interval censoring scheme to the other half. Here the right censoring times were independently simulated from a Uniform(2, 6) distribution. For interval censoring, each subject was assumed to have N observation times, say, O_1, O_2, \dots, O_N , where $(N - 1) \sim \text{Poisson}(2)$ and $(O_k - O_{k-1})|N \stackrel{iid}{\sim} \text{Exp}(1)$ with $O_0 = 0, k = 1, \dots, N$. The observed intervals are the two adjacent observation times (including 0 and ∞) that include the true survival times. The final data yield around 20% right censored, 40% uncensored, 25% left censored and 15% interval censored. For each model, 500 Monte Carlo (MC) replicates were generated. We then fitted each model using the default priors introduced in Section 2.3. For each MCMC algorithm, 5,000 scans were thinned from 50,000 after a burn-in period of 10,000 iterations.

Table 5 summaries the results for regression parameters β and the ICAR variance τ^2 , including the averaged bias (BIAS) and posterior standard deviation (PSD) of each point estimate (posterior mean for β and median for τ^2), the standard deviation (across 500 MC replicates) of the point estimate (SD-Est), the coverage probability (CP) of the 95% creditable interval, and effective sample size (ESS) out of 5,000 (Sargent et al., 2000) for each point estimate. The results show that the point estimates of β and τ^2 are unbiased under all three models, SD-Est values are close to the corresponding PSDs, the CP values are close to the nominal 95% level, and ESS values are promising. Supplementary Figure S1 presents the average, across the 500 MC replicates, of the fitted baseline survival functions and the results reveal that the proposed model is capable to capture complex baseline survival curves very well.

4.2 Simulation II: Comparison

In this section we compare our R function `survregbayes` in the package `spBayesSurv` with R functions `ICBayes` in the package `ICBayes`, `bayessurvreg2` in the package `bayesSurv` and

Table 5: Simulation I. Averaged bias (BIAS) and posterior standard deviation (PSD) of each point estimate, standard deviation (across 500 MC replicates) of the point estimate (SD-Est), coverage probability (CP) for the 95% credible interval, and effective sample size (ESS) out of 5,000 with thinning=10 for each point estimate.

Model	Parameter	BIAS	PSD	SD-Est	CP	ESS
AFT	$\beta_1 = 1$	0.000	0.067	0.062	0.960	3194
	$\beta_2 = 1$	0.002	0.036	0.034	0.960	2992
	$\tau^2 = 1$	0.015	0.311	0.298	0.942	4561
PH	$\beta_1 = 1$	-0.021	0.100	0.099	0.936	3024
	$\beta_2 = 1$	-0.014	0.061	0.060	0.944	2095
	$\tau^2 = 1$	-0.039	0.352	0.319	0.950	3478
PO	$\beta_1 = 1$	0.012	0.151	0.152	0.940	3672
	$\beta_2 = 1$	0.008	0.083	0.086	0.944	2822
	$\tau^2 = 1$	-0.008	0.465	0.448	0.924	2451

`bayesx` in the package `R2BayesX` in terms of mixing and computing speed. Our `survregbayes` can fit all PH, AFT and PO models (either no, IID, ICAR or GRF frailties) for many kind of censored data (either uncensored, interval censored, current status, right censored or arbitrarily censored data). In contrast, `ICBayes` can only fit non-frailty PH and PO models for interval censored data, `bayessurvreg2` can only fit the AFT model (either no or IID frailties), and `bayesx` can only fit the PH model for right-censored data using MCMC. Data are generated from three cases: (C1) the non-frailty PH model with interval censoring, (C2) the non-frailty AFT model with arbitrary censoring, and (C3) the non-frailty PH model with right censoring, where β and S_0 are the same as those used in **Simulation I**. Under each setting we generate 500 MC replicates, each with sample size $n = 500$. For each MCMC run, we retain 10,000 scans without thinning after a burn-in period of 10,000 iterations.

Table 6 reports the comparison results; the ESS from `survregbayes` range from 3 to 20 times as large as those using `ICBayes` and `bayessurvreg2`, indicating that the proposed MCMC algorithms are more efficient in terms of mixing. In addition, `survregbayes` is about 5 times faster than `ICBayes`, although it is much slower than `bayessurvreg2` and `bayesx`. Note that `bayessurvreg2` is almost 9 times faster than our `survregbayes`, but its ESS for β_1 is nearly 19 times smaller than ours. That is, `bayessurvreg2` needs to take 19 times

Table 6: Simulation II. Averaged bias (BIAS) and posterior standard deviation (PSD) of each point estimate, standard deviation (across 500 MC replicates) of the point estimate (SD-Est), coverage probability (CP) for the 95% credible interval, and effective sample size (ESS) out of 10,000 without thinning for each point estimate. The average computing time in seconds is also presented.

Case	R function	Time	Parameter	BIAS	PSD	SD-Est	CP	ESS
C1	survregbayes	63	$\beta_1 = 1$	-0.018	0.134	0.134	0.940	1139
			$\beta_2 = 1$	-0.015	0.086	0.087	0.940	934
	ICBayes	310	$\beta_1 = 1$	-0.036	0.133	0.132	0.938	346
			$\beta_2 = 1$	-0.019	0.084	0.085	0.938	292
C2	survregbayes	54	$\beta_1 = 1$	0.000	0.075	0.074	0.950	1207
			$\beta_2 = 1$	0.002	0.041	0.040	0.952	1186
	bayessurvreg2	6	$\beta_1 = 1$	-0.002	0.072	0.075	0.936	64
			$\beta_2 = 1$	-0.001	0.039	0.040	0.934	109
C3	survregbayes	85	$\beta_1 = 1$	-0.009	0.103	0.061	0.954	1028
			$\beta_2 = 1$	-0.010	0.107	0.061	0.950	673
	bayesx	44	$\beta_1 = 1$	0.017	0.103	0.062	0.940	989
			$\beta_2 = 1$	0.014	0.111	0.064	0.952	2817

more iterates than ours to obtain the same ESS; thus its computing time will be around 120 which is much slower than ours. In comparison with **bayesx** for right censored data, our **survregbayes** performs slightly worse in terms of speed and mixing. This is not surprising, because our MCMC is designed for all AFT, PH and PO with all manner of censoring schemes while the MCMC in **bayesx** is tailored to the PH with right censored data.

Lin et al. (2015) state concerning the **ICBayes** function that “...our developed Gibbs sampler is easy to execute with only four steps and efficient because it does not require imputing any unobserved failure times or contain any complicated Metropolis-Hastings steps.” They further say that their approach is efficient in the sense that their approach is easy to program. However, although the Lin et al. (2015) approach does not require imputing failure times, it does require imputing as many latent Poisson variates as there are spline basis functions *per observation*, i.e. much more latent data than simply imputing the survival times. Furthermore, they update one regression coefficient β_j at a time for $j = 1, \dots, p$ via the ARS

method (Gilks and Wild, 1992), and it is well known that any component-at-a-time sampler will suffer from poor mixing if there is strong correlation in the posterior. The simplest way to improve mixing is through the consideration of adaptive, correlated proposals as we do here. This simulation shows that adaptive block updates can *dramatically* outperform a Gibbs sampler with latent data, both in terms of speed and mixing. The monotone spline approach models the baseline cumulative hazard on the range of the observed data only. The AFT model maps observed data onto “baseline support” through a scale factor; thus only location-scale families can successfully model the AFT. The TBP prior used here circumvents the use of such a static baseline and so our approach is applicable to all of PH, PO, and AFT, as well as accelerated hazards (which also needs a scale term), additive hazards, and proportional mean residual life. Finally, we note that general interval censoring is included in our approach as trivial special cases and does not require separate papers to describe.

5 Discussion

The recent surge in literature analyzing spatially correlated time-to-event data focusing on PH highlights the need for flexible, robust methodology and software to enable the ready use of other competing yet easily-interpretable survival models, spatial or not. An important aspect associated with the Bayesian nonparametric TBP – or more accurately richly parametric – formulation of the AFT, PO, and AFT models presented here is that the assumption of the same flexible prior on S_0 places these models common ground. Differences in fit and/or predictive performance can therefore be attributed to the semiparametric models only, rather than to additional possible differences in quite different nonparametric priors (e.g. gamma process vs. beta process vs. Dirichlet process mixture) or estimation methods (e.g. NPMLE vs. partial likelihood vs. sieves).

Although Cox’s PH model is by far the most commonly-used semiparametric survival model, several studies have shown vastly superior fit and interpretation from AFT and PO

models (Zhou and Hanson, 2015). Cox pointed out himself (Reid, 1994) “...*the physical or substantive basis for...proportional hazards models...is one of its weaknesses...accelerated failure time models are in many ways more appealing because of their quite direct physical interpretation...*” This article provides a unified framework for considering competing models to PH, i.e. AFT and PO, including variable selection, areal or georeferenced frailties, and additive structure. The freely available `survregbayes` function allows for easy fitting of these competing models.

Supplementary Materials

Appendices: Appendix A: MCMC sampling algorithms; Appendix B: brief introduction to the full-scale approximation; Appendix C: definitions of the DIC and LPML criteria; Appendix D: introduction to the R function `survregbayes`; Appendix E: additional results for real data applications; Appendix F: additional simulation results.

References

- Adebayo, S. B. and Fahrmeir, L. (2005). Analysing child mortality in Nigeria with geoaddivitive discrete-time survival models. *Statistics in Medicine*, 24(5):709–728.
- Antoniak, C. E. (1974). Mixtures of Dirichlet processes with applications to Bayesian non-parametric problems. *Annals of Statistics*, 2:1152–1174.
- Arbia, G., Espa, G., Giuliani, D., and Micciolo (2016). A spatial analysis of health and pharmaceutical firm survival. *Journal of Applied Statistics*, page in press.
- Baltazar-Aban, I. and Pena, E. A. (1995). Properties of hazard-based residuals and implications in model diagnostics. *Journal of the American Statistical Association*, 90(429):185–197.

- Banerjee, S., Carlin, B. P., and Gelfand, A. E. (2014). *Hierarchical Modeling and Analysis for Spatial Data, Second Edition*. Chapman and Hall/CRC Press.
- Banerjee, S., Gelfand, A. E., Finley, A. O., and Sang, H. (2008). Gaussian predictive process models for large spatial data sets. *Journal of the Royal Statistical Society: Series B (Statistical Methodology)*, 70(4):825–848.
- Banerjee, S., Wall, M. M., and Carlin, B. P. (2003). Frailty modeling for spatially correlated survival data, with application to infant mortality in Minnesota. *Biostatistics*, 4(1):123–142.
- Belitz, C., Brezger, A., Klein, N., Kneib, T., Lang, S., and Umlauf, N. (2015). BayesX - Software for Bayesian inference in structured additive regression models. Version 3.0. Available from <http://www.bayesx.org>.
- Besag, J. (1974). Spatial interaction and the statistical analysis of lattice systems. *Journal of the Royal Statistical Society: Series B*, 36(2):192–236.
- Bové, D. S., Held, L., et al. (2011). Hyper- g priors for generalized linear models. *Bayesian Analysis*, 6(3):387–410.
- Cai, B., Lin, X., and Wang, L. (2011). Bayesian proportional hazards model for current status data with monotone splines. *Computational Statistics & Data Analysis*, 55(9):2644–2651.
- Chen, Y., Hanson, T., and Zhang, J. (2014). Accelerated hazards model based on parametric families generalized with Bernstein polynomials. *Biometrics*, 70(1):192–201.
- Cox, D. R. (1972). Regression models and life-tables (with discussion). *Journal of the Royal Statistical Society. Series B (Methodological)*, 34(2):187–220.
- Cox, D. R. and Oakes, D. (1984). *Analysis of Survival Data*. Chapman & Hall: London.
- Cox, D. R. and Snell, E. J. (1968). A general definition of residuals. *Journal of the Royal Statistical Society. Series B (Methodological)*, 30(2):248–275.

- Cressie, N. and Johannesson, G. (2008). Fixed rank kriging for very large spatial data sets. *Journal of the Royal Statistical Society: Series B (Statistical Methodology)*, 70(1):209–226.
- Darmofal, D. (2009). Bayesian spatial survival models for political event processes. *American Journal of Political Science*, 53(1):241–257.
- Dickey, J. M. (1971). The weighted likelihood ratio, linear hypotheses on normal location parameters. *The Annals of Mathematical Statistics*, 42(1):204–223.
- Diva, U., Dey, D. K., and Banerjee, S. (2008). Parametric models for spatially correlated survival data for individuals with multiple cancers. *Statistics in Medicine*, 27(12):2127–2144.
- Fahrmeir, L. and Kneib, T. (2011). *Bayesian Smoothing and Regression for Longitudinal, Spatial and Event History Data*. Oxford University Press.
- Ferguson, T. S. (1973). A Bayesian analysis of some nonparametric problems. *The Annals of Statistics*, 1:209–230.
- Geisser, S. and Eddy, W. F. (1979). A predictive approach to model selection. *Journal of the American Statistical Association*, 74(365):153–160.
- Gilks, W. R. and Wild, P. (1992). Adaptive rejection sampling for Gibbs sampling. *Applied Statistics*, pages 337–348.
- Gray, R. J. (1992). Flexible methods for analyzing survival data using splines, with applications to breast cancer prognosis. *Journal of the American Statistical Association*, 87:942–951.
- Haario, H., Saksman, E., and Tamminen, J. (2001). An adaptive Metropolis algorithm. *Bernoulli*, 7(2):223–242.
- Hanson, T., Johnson, W., and Laud, P. (2009). Semiparametric inference for survival models with step process covariates. *Canadian Journal of Statistics*, 37(1):60–79.

- Hanson, T. E., Branscum, A. J., Johnson, W. O., et al. (2014). Informative g -priors for logistic regression. *Bayesian Analysis*, 9(3):597–612.
- Hanson, T. E., Jara, A., Zhao, L., et al. (2012). A Bayesian semiparametric temporally-stratified proportional hazards model with spatial frailties. *Bayesian Analysis*, 7(1):147–188.
- Henderson, R., Shimakura, S., and Gorst, D. (2002). Modeling spatial variation in leukemia survival data. *Journal of the American Statistical Association*, 97(460):965–972.
- Hennerfeind, A., Brezger, A., and Fahrmeir, L. (2006). Geoaddivitive survival models. *Journal of the American Statistical Association*, 101(475):1065–1075.
- Higdon, D. (2002). Space and space-time modeling using process convolutions. In *Quantitative methods for current environmental issues*, pages 37–56. Springer.
- Jerrett, M., Burnett, R. T., Beckerman, B. S., Turner, M. C., Krewski, D., Thurston, G., Martin, R. V., van Donkelaar, A., Hughes, E., Shi, Y., Gapstur, S. M., Thun, M. J., and Pope, C. A. (2013). Spatial analysis of air pollution and mortality in California. *American Journal of Respiratory and Critical Care Medicine*, 188:593–599.
- Kalbfleisch, J. (1978). Non-parametric Bayesian analysis of survival time data. *Journal of the Royal Statistical Society, Series B*, 40(2):214–221.
- Kamman, E. E. and Wand, M. P. (2003). Geoaddivitive models. *Applied Statistics*, 52:1–18.
- Kaufman, C. G., Schervish, M. J., and Nychka, D. W. (2008). Covariance tapering for likelihood-based estimation in large spatial data sets. *Journal of the American Statistical Association*, 103(484):1545–1555.
- Kneib, T. (2006). Mixed model-based inference in geoaddivitive hazard regression for interval-censored survival times. *Computational Statistics & Data Analysis*, 51(2):777–792.

- Kneib, T. and Fahrmeir, L. (2007). A mixed model approach for geoadditive hazard regression. *Scandinavian Journal of Statistics*, 34(1):207–228.
- Komarek, A. (2006). *Accelerated failure time models for multivariate interval-censored data with flexible distributional assumptions*. PhD thesis, PhD thesis, Katholieke Universiteit Leuven, Faculteit Wetenschappen.
- Komárek, A. and Lesaffre, E. (2008). Bayesian accelerated failure time model with multivariate doubly-interval-censored data and flexible distributional assumptions. *Journal of the American Statistical Association*, 103:523–533.
- Komárek, A. and Lesaffre, E. (2009). The regression analysis of correlated interval-censored data illustration using accelerated failure time models with flexible distributional assumptions. *Statistical Modelling*, 9(4):299–319.
- Kuo, L. and Mallick, B. (1998). Variable selection for regression models. *Sankhyā: The Indian Journal of Statistics, Series B*, 60:65–81.
- Lavine, M. (1992). Some aspects of Polya tree distributions for statistical modelling. *The Annals of Statistics*, 20:1222–1235.
- Li, J., Hong, Y., Thapa, R., and Burkhart, H. E. (2015a). Survival analysis of loblolly pine trees with spatially correlated random effects. *Journal of the American Statistical Association*, 110(510):486–502.
- Li, L., Hanson, T., and Zhang, J. (2015b). Spatial extended hazard model with application to prostate cancer survival. *Biometrics*, 71(2):313–322.
- Li, Y. and Lin, X. (2006). Semiparametric normal transformation models for spatially correlated survival data. *Journal of the American Statistical Association*, 101(474):591–603.
- Li, Y. and Ryan, L. (2002). Modeling spatial survival data using semiparametric frailty models. *Biometrics*, 58(2):287–297.

- Lin, X., Cai, B., Wang, L., and Zhang, Z. (2015). A Bayesian proportional hazards model for general interval-censored data. *Lifetime Data Analysis*, 21(3):470–490.
- Lin, X. and Wang, L. (2011). Bayesian proportional odds models for analyzing current status data: univariate, clustered, and multivariate. *Communications in Statistics-Simulation and Computation*, 40(8):1171–1181.
- Liu, J., Sui, X., Lavie, C. J., Zhou, H., Park, Y.-M. M., Cai, B., Liu, J., and Blair, S. N. (2014). Effects of cardiorespiratory fitness on blood pressure trajectory with aging in a cohort of healthy men. *Journal of the American College of Cardiology*, 64(12):1245–1253.
- Martins, R., Silva, G. L., and Andreozzi, V. (2016). Bayesian joint modeling of longitudinal and spatial survival aids data. *Statistics in Medicine*, 35:3368–3384.
- Morin, A. A. (2014). A Spatial Analysis of Forest Fire Survival and a Marked Cluster Process for Simulating Fire Load. Master’s thesis, The University of Western Ontario, London, Ontario, Canada.
- Müller, P., Quintana, F., Jara, A., and Hanson, T. (2015). *Bayesian Nonparametric Data Analysis*. Springer-Verlag: New York.
- Nardi, A. and Schemper, M. (2003). Comparing Cox and parametric models in clinical studies. *Statistics in Medicine*, 22(23):3597–3610.
- National Population Commission (NPC) [Nigeria] and ORC Macro (2004). *Nigeria Demographic and Health Survey 2003*. Calverton, Maryland: National Population Commission and ORC Macro.
- O’Hara, R. B., Sillanpää, M. J., et al. (2009). A review of Bayesian variable selection methods: what, how and which. *Bayesian Analysis*, 4(1):85–118.
- Ojiambo, P. and Kang, E. (2013). Modeling spatial frailties in survival analysis of cucurbit downy mildew epidemics. *Phytopathology*, 103(3):216–227.

- O’Quigley, J. and Xu, R. (2005). Goodness of fit in survival analysis. In *Encyclopedia of Biostatistics*. John Wiley & Sons, Ltd.
- Pan, C., Cai, B., Wang, L., and Lin, X. (2014). Bayesian semiparametric model for spatially correlated interval-censored survival data. *Computational Statistics & Data Analysis*, 74:198–209.
- Pan, C., Cai, B., Wang, L., and Lin, X. (2015). *ICBayes: Bayesian Semiparametric Models for Interval-Censored Data*. R package version 1.0.
- Petrone, S. (1999). Random Bernstein polynomials. *Scandinavian Journal of Statistics*, 26:373–393.
- Petrone, S. and Wasserman, L. (2002). Consistency of bernstein polynomial posteriors. *Journal of the Royal Statistical Society: Series B (Statistical Methodology)*, 64(1):79–100.
- Prentice, R. L. and Kalbfleisch, J. D. (1979). Hazard rate models with covariates. *Biometrics*, 35:25–39.
- Reid, N. (1994). A conversation with Sir David Cox. *Statistical Science*, 9:439–455.
- Sang, H. and Huang, J. Z. (2012). A full scale approximation of covariance functions for large spatial data sets. *Journal of the Royal Statistical Society: Series B (Statistical Methodology)*, 74(1):111–132.
- Sargent, D. J., Hodges, J. S., and Carlin, B. P. (2000). Structured Markov chain Monte Carlo. *Journal of Computational and Graphical Statistics*, 9(2):217–234.
- Schnell, P., Bandyopadhyay, D., Reich, B. J., and Nunn, M. (2015). A marginal cure rate proportional hazards model for spatial survival data. *Journal of the Royal Statistical Society: Series C (Applied Statistics)*, 64(4):673–691.

- Spiegelhalter, D. J., Best, N. G., Carlin, B. P., and Van Der Linde, A. (2002). Bayesian measures of model complexity and fit. *Journal of the Royal Statistical Society, Series B*, 64(4):583–639.
- Taylor, B. M. (2016). Spatial modelling of emergency service response times. *Journal of the Royal Statistical Society: Series A (Statistics in Society)*, in press.
- Turnbull, B. W. (1974). Nonparametric estimation of a survivorship function with doubly censored data. *Journal of the American Statistical Association*, 69(345):169–173.
- Umlauf, N., Adler, D., Kneib, T., Lang, S., and Zeileis, A. (2015). Structured additive regression models: An R interface to BayesX. *Journal of Statistical Software*, 63(21):1–46.
- Verdinelli, I. and Wasserman, L. (1995). Computing Bayes factors using a generalization of the Savage-Dickey density ratio. *Journal of the American Statistical Association*, 90(430):614–618.
- Wang, L. and Lin, X. (2011). A Bayesian approach for analyzing case 2 interval-censored failure time data under the semiparametric proportional odds model. *Statistics & Probability Letters*, 81:876–883.
- Wang, L., McMahan, C. S., Hudgens, M. G., and Qureshi, Z. P. (2016). A flexible, computationally efficient method for fitting the proportional hazards model to interval-censored data. *Biometrics*, 72(1):222–231.
- Wang, S., Zhang, J., and Lawson, A. B. (2012). A Bayesian normal mixture accelerated failure time spatial model and its application to prostate cancer. *Statistical Methods in Medical Research*, <http://dx.doi.org/10.1177/0962280212466189>.
- Zellner, A. (1983). Applications of Bayesian analysis in econometrics. *The Statistician*, 32:23–34.

- Zhao, L. and Hanson, T. E. (2011). Spatially dependent Polya tree modeling for survival data. *Biometrics*, 67(2):391–403.
- Zhao, L., Hanson, T. E., and Carlin, B. P. (2009). Mixtures of Polya trees for flexible spatial frailty survival modelling. *Biometrika*, 96(2):263–276.
- Zhou, H. and Hanson, T. (2015). Bayesian spatial survival models. In *Nonparametric Bayesian Inference in Biostatistics*, pages 215–246. Springer.
- Zhou, H. and Hanson, T. (2016). *spBayesSurv: Bayesian Modeling and Analysis of Spatially Correlated Survival Data*. R package version 1.0.6.
- Zhou, H., Hanson, T., Jara, A., and Zhang, J. (2015). Modeling county level breast cancer survival data using a covariate-adjusted frailty proportional hazards model. *The Annals of Applied Statistics*, 9(1):43–68.
- Zhou, H., Hanson, T., and Zhang, J. (2016). Generalized accelerated failure time spatial frailty model for arbitrarily censored data. *Lifetime Data Analysis*, in press.

Supplementary Materials for “*A unified framework for fitting Bayesian semiparametric models to arbitrarily censored spatial survival data*” by Haiming Zhou and Timothy Hanson

Appendix A MCMC Sampling

The joint posterior distribution for all parameters is given by

$$\begin{aligned}
 \mathcal{L}(\boldsymbol{\beta}, \boldsymbol{\theta}, \mathbf{w}_J, \alpha, \mathbf{v}, \tau^2, \phi) &\propto L(\mathbf{w}_J, \boldsymbol{\theta}, \boldsymbol{\beta}, \mathbf{v}) \\
 &\times \exp \left\{ -\frac{1}{2}(\boldsymbol{\beta} - \boldsymbol{\beta}_0)' \mathbf{S}_0^{-1}(\boldsymbol{\beta} - \boldsymbol{\beta}_0) \right\} \\
 &\times \exp \left\{ -\frac{1}{2}(\boldsymbol{\theta} - \boldsymbol{\theta}_0)' \mathbf{V}_0^{-1}(\boldsymbol{\theta} - \boldsymbol{\theta}_0) \right\} \\
 &\times \frac{\Gamma(\alpha J)}{\Gamma(\alpha)^J} \prod_{j=1}^J (w_j)^{\alpha-1} \times \alpha^{a_0-1} \exp\{-b_0 \alpha\} \\
 &\times (\tau^{-2})^{\frac{\text{rank}(\mathbf{K})}{2}} \exp \left\{ -\frac{1}{2\tau^2} \mathbf{v}' \mathbf{K} \mathbf{v} \right\} \times (\tau^{-2})^{a_\tau-1} \exp\{-b_\tau \tau^{-2}\} \\
 &\times p(\phi) |\mathbf{K}|^{1/2}
 \end{aligned} \tag{A.1}$$

Here for georeferenced data, $\mathbf{K} = \mathbf{R}^{-1}$ and $p(\phi) = \phi^{a_\phi-1} \exp\{-b_\phi \phi\}$. For areal data, $p(\phi) |\mathbf{R}|^{-1/2}$ is not needed, and $\mathbf{K} = \mathbf{D}_e - \mathbf{E}$, where \mathbf{D}_e is an $m \times m$ diagonal matrix with $\mathbf{D}_e[i, i] = e_{i+}$.

Note that when $w_j = 1/J$ the underlying parametric model with $S_0(t) = S_\theta(t)$ is obtained, so a fit from a standard parametric survival model can provide starting values for the TBP survival model. Let $\hat{\boldsymbol{\theta}}$ and $\hat{\boldsymbol{\beta}}$ denote the parametric point estimates of $\boldsymbol{\theta}$ and $\boldsymbol{\beta}$, and let $\hat{\mathbf{V}}$ and $\hat{\mathbf{S}}$ denote their asymptotic covariance matrices, respectively. These estimates can be easily obtained by running the proposed MCMC below with $w_j \equiv 1/J$ and relative vague priors on $(\boldsymbol{\theta}, \boldsymbol{\beta})$.

Step 1: Update \mathbf{w}_J .

Set $\mathbf{z}_{J-1} = (z_1, \dots, z_{J-1})'$ with $z_j = \log(w_j) - \log(w_J)$. It follows that the full conditional distribution for \mathbf{z}_{J-1} is

$$p(\mathbf{z}_{J-1} | \text{else}) \propto L(\mathbf{w}_J, \boldsymbol{\theta}, \boldsymbol{\beta}, \mathbf{v}) \times \prod_{j=1}^J \left[\frac{e^{z_j}}{\sum_{k=1}^J e^{z_k}} \right]^\alpha,$$

where $z_J = 0$. The vector \mathbf{z}_{J-1} can be updated using adaptive Metropolis samplers (Haario et al., 2001). Suppose we are currently in iteration l and have sampled the states $\mathbf{z}_{J-1}^{(1)}, \dots, \mathbf{z}_{J-1}^{(l-1)}$. We

select an index l_0 (e.g., $l_0 = 5000$) for the length of an initial period and define

$$\Sigma_l = \begin{cases} \Sigma_0, & l \leq l_0 \\ \frac{(2.4)^2}{d}(\mathcal{C}_l + 10^{-10}\mathbf{I}_d) & l > l_0. \end{cases}$$

Here \mathcal{C}_l is the sample variance of $\mathbf{z}_{J-1}^{(1)}, \dots, \mathbf{z}_{J-1}^{(l-1)}$, $d = J - 1$ is the dimension of \mathbf{z}_{J-1} , and Σ_0 is an initial diagonal covariance matrix of \mathbf{z} , defined so that the variance of z_j is 0.16. The choice of 0.16 is based on our extensive simulation studies; other choices (as long as it is not too small or large) will have little impact on posterior inferences. We generate $\mathbf{z}_{J-1}^* = (z_1^*, \dots, z_{J-1}^*)'$ from $N_{J-1}(\mathbf{z}_{J-1}^{(l-1)}, \Sigma_l)$ and accept it with probability

$$\min \left\{ 1, \frac{p(\mathbf{z}_{J-1}^*|\text{else})}{p(\mathbf{z}_{J-1}^{(l-1)}|\text{else})} \right\}.$$

Step 2: Update $\boldsymbol{\theta}$.

The full conditional distribution for $\boldsymbol{\theta}$ is

$$p(\boldsymbol{\theta}|\text{else}) \propto L(\mathbf{w}_J, \boldsymbol{\theta}, \boldsymbol{\beta}, \mathbf{v}) \times \exp \left\{ -\frac{1}{2}(\boldsymbol{\theta} - \boldsymbol{\theta}_0)' \mathbf{V}_0^{-1}(\boldsymbol{\theta} - \boldsymbol{\theta}_0) \right\}.$$

The centering distribution parameters $\boldsymbol{\theta}$ are updated via adaptive Metropolis samplers. At iteration l , each candidate is sampled as $\boldsymbol{\theta}^* \sim N_2(\boldsymbol{\theta}^{(l-1)}, \Sigma_l)$ and accepted with probability

$$\min \left\{ 1, \frac{p(\boldsymbol{\theta}^*|\text{else})}{p(\boldsymbol{\theta}^{(l-1)}|\text{else})} \right\}.$$

where $\phi_2(\cdot|\boldsymbol{\theta}_0, \mathbf{V}_0)$ denotes the density of $N_2(\boldsymbol{\theta}_0, \mathbf{V}_0)$, and Σ_l is defined similarly as above, but with Σ_0 set to be $\hat{\mathbf{V}}$.

Step 3: Update $\boldsymbol{\beta}$.

The full conditional distribution for $\boldsymbol{\beta}$ is

$$p(\boldsymbol{\theta}|\text{else}) \propto L(\mathbf{w}_J, \boldsymbol{\theta}, \boldsymbol{\beta}, \mathbf{v}) \times \exp \left\{ -\frac{1}{2}(\boldsymbol{\beta} - \boldsymbol{\beta}_0)' \mathbf{S}_0^{-1}(\boldsymbol{\beta} - \boldsymbol{\beta}_0) \right\}.$$

The survival model coefficients $\boldsymbol{\beta}$ are updated via adaptive Metropolis samplers as well with proposal $\boldsymbol{\beta}^* \sim N_p(\boldsymbol{\beta}^{(l-1)}, \Sigma_l)$ and acceptance probability

$$\min \left\{ 1, \frac{p(\boldsymbol{\beta}^*|\text{else})}{p(\boldsymbol{\beta}^{(l-1)}|\text{else})} \right\}.$$

where Σ_l is defined similarly as above with $\Sigma_0 = \hat{\mathbf{S}}$.

Step 4: Update α .

The full conditional distribution for α is

$$p(\alpha|\text{else}) \propto \frac{\Gamma(\alpha J)}{\Gamma(\alpha)^J} \prod_{j=1}^J (w_j)^{\alpha-1} \times \alpha^{a_0-1} \exp\{-b_0\alpha\}.$$

The precision parameter α is updated via adaptive Metropolis samplers with normal proposal $\alpha^* \sim N_1(\alpha^{(l-1)}, \mathbf{\Sigma}_l)$ with $\mathbf{\Sigma}_l$ is defined similarly as above with $\mathbf{\Sigma}_0 = 0.16$, and the acceptance probability is

$$\min \left\{ 1, \frac{p(\alpha^*|\text{else})}{p(\alpha^{(l-1)}|\text{else})} \right\}.$$

Step 5: Update \mathbf{v} .

Let $L(\mathbf{w}_J, \boldsymbol{\theta}, \boldsymbol{\beta}, \mathbf{v}) = \prod_{i=1}^m \prod_{j=1}^{n_i} L_{ij}(\mathbf{w}_J, \boldsymbol{\theta}, \boldsymbol{\beta}, \mathbf{v})$. For areal data, the full conditional distribution for v_i , $i = 1, \dots, m$, is

$$p(v_i|\text{else}) \propto \prod_{j=1}^{n_i} L_{ij}(\mathbf{w}_J, \boldsymbol{\theta}, \boldsymbol{\beta}, \mathbf{v}) \exp \left\{ -\frac{e_{i+}}{2\tau^2} \left(v_i - \sum_{j=1}^m e_{ij}v_j/e_{i+} \right)^2 \right\}.$$

The v_j is updated via Metropolis-Hastings sampling steps with proposal $v_j^* \sim N(v_j^{(l-1)}, \tau^2/e_{j+})$. The candidate v_j^* is accepted with probability

$$\min \left\{ 1, \frac{p(v_j^*|\text{else})}{p(v_j^{(l-1)}|\text{else})} \right\}.$$

For georeferenced data, the full conditional distribution for v_i , $i = 1, \dots, m$, is

$$p(v_i|\text{else}) \propto \prod_{j=1}^{n_i} L_{ij}(\mathbf{w}_J, \boldsymbol{\theta}, \boldsymbol{\beta}, \mathbf{v}) \exp \left\{ -\frac{p_{ii}}{2\tau^2} \left(v_i + \sum_{\{j:j \neq i\}} p_{ij}v_j/p_{ii} \right)^2 \right\},$$

where p_{ij} is the (i, j) element of \mathbf{R}^{-1} . The v_j is updated via Metropolis-Hastings sampling steps with proposal $v_j^* \sim N(v_j^{(l-1)}, \tau^2/p_{ii})$. The candidate v_j^* is accepted with probability

$$\min \left\{ 1, \frac{p(v_j^*|\text{else})}{p(v_j^{(l-1)}|\text{else})} \right\}.$$

Step 6: Update τ^2 .

The full conditional distribution for τ^{-2} is

$$p(\tau^{-2}|\text{else}) \propto (\tau^{-2})^{a_\tau + \frac{\text{rank}(\mathbf{K})}{2} - 1} \exp \left\{ -\left[b_\tau + \frac{1}{2} \mathbf{v}' \mathbf{K} \mathbf{v} \right] \tau^{-2} \right\}.$$

Thus τ^{-2} is sampled from $\Gamma(a_\tau^*, b_\tau^*)$, where $a_\tau^* = a_\tau + \frac{\text{rank}(\mathbf{K})}{2} - 1$ and $b_\tau^* = b_\tau + \frac{1}{2} \mathbf{v}' \mathbf{K} \mathbf{v}$.

Step 7: Update ϕ for georeferenced data.

The full conditional distribution for ϕ is

$$p(\phi|\text{else}) \propto |\mathbf{R}|^{-1/2} \exp \left\{ -\frac{1}{2\tau^2} \mathbf{v}' \mathbf{R}^{-1} \mathbf{v} \right\} \phi^{a_\tau - 1} \exp \{ -b_\phi \phi \}$$

The range parameter ϕ is updated via adaptive Metropolis samplers with normal proposal $\phi^* \sim N_1(\phi^{(l-1)}, \mathbf{\Sigma}_l)$ with $\mathbf{\Sigma}_l$ is defined similarly as above with $\mathbf{\Sigma}_0 = 0.16$, and the acceptance probability is

$$\min \left\{ 1, \frac{p(\phi^*|\text{else})}{p(\phi^{(l-1)}|\text{else})} \right\}.$$

Step 8: Update γ when variable selection is performed.

When variable selection is performed, all β s in steps 1-7 need to be replaced by $\gamma \odot \beta$, where \odot denotes componentwise multiplication. Then each γ_j is generated from its full conditional, i.e. a Bernoulli distribution with the success probability

$$\frac{q_j}{q_j + (1 - q_j)L(\mathbf{w}_J, \boldsymbol{\theta}, \gamma_{j0} \odot \beta, \mathbf{v}) / L(\mathbf{w}_J, \boldsymbol{\theta}, \gamma_{j1} \odot \beta, \mathbf{v})},$$

where the vector γ_{j0} (γ_{j1}) is obtained from γ with the j th element replaced by 0 (1).

Appendix B The Full Scale Approximation

For georeferenced data, a computational bottleneck of the MCMC sampling scheme is inverting the $m \times m$ matrix \mathbf{R} , which typically has computational cost $O(m^3)$. In this section, we introduce a full scale approximation (FSA) approach proposed by Sang and Huang (2012), which provides a high quality approximation to the correlation function ρ at both the large and the small spatial scales, such that the inverse of \mathbf{R} can be substantially sped up for large value of m , e.g., $m \geq 500$.

Consider a fixed set of “knots” $\mathcal{S}^* = \{\mathbf{s}_1^*, \dots, \mathbf{s}_K^*\}$ chosen from the study region. These knots can be chosen using the function `cover.design` within the R package `fields`, which computes space-filling coverage designs using the swapping algorithm (Johnson et al., 1990). Let $\rho(\mathbf{s}, \mathbf{s}')$ be the correlation between locations \mathbf{s} and \mathbf{s}' . The FSA approach approximates the correlation function $\rho(\mathbf{s}, \mathbf{s}')$ with

$$\rho^\dagger(\mathbf{s}, \mathbf{s}') = \rho_l(\mathbf{s}, \mathbf{s}') + \rho_s(\mathbf{s}, \mathbf{s}'). \quad (\text{B.2})$$

The $\rho_l(\mathbf{s}, \mathbf{s}')$ in (B.2) is the reduced-rank part capturing the long-scale spatial dependence, defined as $\rho_l(\mathbf{s}, \mathbf{s}') = \rho'(\mathbf{s}, \mathcal{S}^*) \rho_{KK}^{-1}(\mathcal{S}^*, \mathcal{S}^*) \rho(\mathbf{s}', \mathcal{S}^*)$, where $\rho(\mathbf{s}, \mathcal{S}^*) = [\rho(\mathbf{s}, \mathbf{s}_i^*)]_{i=1}^K$ is an $K \times 1$ vector, and $\rho_{KK}(\mathcal{S}^*, \mathcal{S}^*) = [\rho(\mathbf{s}_i^*, \mathbf{s}_j^*)]_{i,j=1}^K$ is an $K \times K$ correlation matrix at knots \mathcal{S}^* . However, $\rho_l(\mathbf{s}, \mathbf{s}')$ cannot well capture the short-scale dependence due to the fact that it discards entirely the residual part $\rho(\mathbf{s}, \mathbf{s}') - \rho_l(\mathbf{s}, \mathbf{s}')$. The idea of FSA is to add a small-scale part $\rho_s(\mathbf{s}, \mathbf{s}')$ as a sparse approximate of the residual part, defined by $\rho_s(\mathbf{s}, \mathbf{s}') = \{\rho(\mathbf{s}, \mathbf{s}') - \rho_l(\mathbf{s}, \mathbf{s}')\} \Delta(\mathbf{s}, \mathbf{s}')$, where $\Delta(\mathbf{s}, \mathbf{s}')$ is a modulating function, which is specified so that the $\rho_s(\mathbf{s}, \mathbf{s}')$ can well capture the local residual spatial dependence while still permits efficient computations. Motivated by Konomi et al. (2014), we first partition the total input space into B disjoint blocks, and then specify $\Delta(\mathbf{s}, \mathbf{s}')$ in a way such that the residuals are independent across input blocks, but the original residual dependence structure within each block is retained. Specifically, the function $\Delta(\mathbf{s}, \mathbf{s}')$ is taken to be 1 if \mathbf{s} and \mathbf{s}' belong to the same block and 0 otherwise. The approximated correlation function $\rho^\dagger(\mathbf{s}, \mathbf{s}')$ in (B.2) provides an exact recovery of the true correlation within each block, and the approximation errors are $\rho(\mathbf{s}, \mathbf{s}') - \rho_l(\mathbf{s}, \mathbf{s}')$ for locations \mathbf{s} and \mathbf{s}' in different blocks. Those errors are expected to be small for most entries because most of these location pairs are farther apart. To determine the blocks, we first use the R function `cover.design` to choose $B \leq m$ locations among the m locations forming B blocks, then assign each \mathbf{s}_i to the block that is closest to \mathbf{s}_i . Here B does not need to be equal to K . When $B = 1$, no approximation is applied to the correlation ρ . When $B = m$, it reduces to the approach of Finley et al. (2009), so the local residual spatial dependence may not be well captured.

Applying the above FSA approach to approximate the correlation function $\rho(\mathbf{s}, \mathbf{s}')$, we can approximate the correlation matrix \mathbf{R} with

$$\boldsymbol{\rho}_{mm}^\dagger = \boldsymbol{\rho}_l + \boldsymbol{\rho}_s = \boldsymbol{\rho}_{mK} \boldsymbol{\rho}_{KK}^{-1} \boldsymbol{\rho}_{mK}' + (\boldsymbol{\rho}_{mm} - \boldsymbol{\rho}_{mK} \boldsymbol{\rho}_{KK}^{-1} \boldsymbol{\rho}_{mK}') \circ \boldsymbol{\Delta}, \quad (\text{B.3})$$

where $\boldsymbol{\rho}_{mK} = [\rho(\mathbf{s}_i, \mathbf{s}_j^*)]_{i=1:m, j=1:K}$, $\boldsymbol{\rho}_{KK} = [\rho(\mathbf{s}_i^*, \mathbf{s}_j^*)]_{i,j=1}^K$, and $\boldsymbol{\Delta} = [\Delta(\mathbf{s}_i, \mathbf{s}_j)]_{i,j=1}^m$. Here, the notation “ \circ ” represents the element-wise matrix multiplication. To avoid numerical instability, we

add a small nugget effect $\epsilon = 0.001$ when define \mathbf{R} , that is, $\mathbf{R} = (1 - \epsilon)\boldsymbol{\rho}_{mm} + \epsilon\mathbf{I}_m$. It follows from equation (B.3) that \mathbf{R} can be approximated by

$$\mathbf{R}^\dagger = (1 - \epsilon)\boldsymbol{\rho}_{mm}^\dagger + \epsilon\mathbf{I}_m = (1 - \epsilon)\boldsymbol{\rho}_{mK}\boldsymbol{\rho}_{KK}^{-1}\boldsymbol{\rho}_{mK}' + \mathbf{R}_s,$$

where $\mathbf{R}_s = (1 - \epsilon)(\boldsymbol{\rho}_{mm} - \boldsymbol{\rho}_{mK}\boldsymbol{\rho}_{KK}^{-1}\boldsymbol{\rho}_{mK}') \circ \boldsymbol{\Delta} + \epsilon\mathbf{I}_m$. Applying the Sherman-Woodbury-Morrison formula for inverse matrices, we can approximate \mathbf{R}^{-1} by

$$(\mathbf{R}^\dagger)^{-1} = \mathbf{R}_s^{-1} - (1 - \epsilon)\mathbf{R}_s^{-1}\boldsymbol{\rho}_{mK}[\boldsymbol{\rho}_{KK} + (1 - \epsilon)\boldsymbol{\rho}_{mK}'\mathbf{R}_s^{-1}\boldsymbol{\rho}_{mK}]^{-1}\boldsymbol{\rho}_{mK}'\mathbf{R}_s^{-1}. \quad (\text{B.4})$$

In addition, the determinant of \mathbf{R} can be approximated by

$$\det(\mathbf{R}^\dagger) = \det\{\boldsymbol{\rho}_{KK} + (1 - \epsilon)\boldsymbol{\rho}_{mK}'\mathbf{R}_s^{-1}\boldsymbol{\rho}_{mK}\} \det(\boldsymbol{\rho}_{KK})^{-1} \det(\mathbf{R}_s). \quad (\text{B.5})$$

Since the $m \times m$ matrix \mathbf{R}_s is a block matrix, the right-hand sides of equations (B.4) and (B.5) involve only inverses and determinants of $K \times K$ low-rank matrices and $m \times m$ block diagonal matrices. Thus the computational complexity can be greatly reduced relative to the expensive computational cost of using original correlation function for large value of m .

Appendix C The DIC and LPML Criteria

The DIC, a generalization of the Akaike information criterion (AIC), is commonly used for comparing complex hierarchical models for which the asymptotic justification of AIC is not appropriate. Let Ω denote the entire collection of model parameters under a particular model and $f(\mathcal{D}|\Omega)$ is the likelihood function based on observed data \mathcal{D} . The DIC is defined

$$\text{DIC} = E_{\Omega|\mathcal{D}}[D(\Omega)] + p_D \quad (\text{C.6})$$

where $D(\Omega) = -2 \log f(\mathcal{D}|\Omega)$ which is referred to as the deviance function, and $p_D = E_{\Omega|\mathcal{D}}[D(\Omega)] - D(E_{\Omega|\mathcal{D}}[\Omega])$ which is the effective number of parameters measuring the model complexity. Similar to AIC, a smaller value of DIC indicates a better fit model.

The definition of LPML is based on the conditional predictive ordinate (CPO) statistic. Let $f_1(\cdot)$ and $f_2(\cdot)$ denote likelihood functions corresponding to models 1 and 2, respectively. The CPO for observation i under model k is given by

$$\text{CPO}_{i,k} = f_k(\mathcal{D}_i|\mathcal{D}_{-i}),$$

where \mathcal{D}_{-i} is the dataset with the i th data point removed. The ratio $\text{CPO}_{i,1}/\text{CPO}_{i,2}$ measures how well model 1 supports the observation \mathcal{D}_i relative to model 2, based on the remaining data \mathcal{D}_{-i} . The product of the CPO ratios gives an overall aggregate summary of how well supported the data are by model 1 relative to model 2 and is called the pseudo Bayes factor (PBF),

$$B_{12} = \prod_{i=1}^n \frac{\text{CPO}_{i,1}}{\text{CPO}_{i,2}}.$$

It is well known that Bayes factors (Kass and Raftery, 1995; Han and Carlin, 2001) are usually difficult to obtain in practice. The PBF is a surrogate for the more traditional Bayes factor and can be interpreted similarly, but is more analytically tractable, much less sensitive to prior assumptions, and does not suffer from Lindley's paradox. Finally, the LPML statistic for model k is defined as $\text{LPML}_k = \log \prod_{i=1}^n \text{CPO}_{i,k}$, and therefore $B_{12} = \exp(\text{LPML}_1 - \text{LPML}_2)$.

Appendix D Implementation Using R

We present how to use the R function `survregbayes` in the package `spBayesSurv` to fit the AFT, PH and PO frailty models with the transformed Bernstein polynomials (TBP) prior on baseline survival functions using simulated data. We take Example 2 of the variable selection simulation (see **Simulation IV** below) as an example. The following code is used to generate data:

```
##-----Load libraries-----##
rm(list=ls())
library(coda)
library(survival)
library(spBayesSurv)

##-----Set the true models-----##
betaT = c(1,1,0,0,0);
## Baseline Survival
f0oft = function(t) 0.5*dlnorm(t, -1, 0.5)+0.5*dlnorm(t,1,0.5);
S0oft = function(t) 0.5*plnorm(t, -1, 0.5, lower.tail=FALSE)+
0.5*plnorm(t, 1, 0.5, lower.tail=FALSE)
## The Survival function:
Sioft = function(t,x,v=0) exp( log(S0oft(t))*exp(sum(x*betaT)+v) );
Fioft = function(t,x,v=0) 1-Sioft(t,x,v);
## The inverse for Fioft
Finv = function(u, x,v=0) uniroot(function (t) Fioft(t,x,v)-u, lower=1e-100, upper=1e100,
extendInt = "yes")$root

##-----Generate data-----##
## read the adjacency matrix of Nigeria for the 37 states
m=37;
W = matrix(scan("adjacency.txt"), m, m);
tau2T = 1;
covT = tau2T*solve(diag(rowSums(W))-W+diag(rep(1e-10, m)));
v0 = MASS::mvrnorm(n=1, mu=rep(0,m), Sigma=covT);
v = v0-mean(v0);
mis = rep(20, m); n = sum(mis);
vn = rep(v, mis);
id = rep(1:m, mis);
## generate x
x1 = rbinom(n, 1, 0.5); x2 = rnorm(n, 0, 1);
x3 = x2+0.15*rnorm(n); x4 = rnorm(n, 0, 1); x5 = rnorm(n, 0, 1);
X = cbind(x1, x2, x3, x4, x5);
colnames(X) = c("x1", "x2", "x3", "x4", "x5");
## generate survival times
u = runif(n);
tT = rep(0, n);
for (i in 1:n){
tT[i] = Finv(u[i], X[i,], vn[i]);
}
## generate partly interval-censored data
t1=rep(NA, n);t2=rep(NA, n); delta=rep(NA, n);
n1 = floor(0.5*n); ## right-censored part
n2 = n-n1; ## interval-censored part
# right-censored part
rcen = sample(1:n, n1);
t1_r=tT[rcen];t2_r=tT[rcen];
Centime = runif(n1, 2, 6);
delta_r = (tT[rcen]<=Centime) +0 ; length(which(delta_r==0))/n1;
t1_r[which(delta_r==0)] = Centime[which(delta_r==0)];
```

```

t2_r[which(delta_r==0)] = NA;
t1[rcen]=t1_r; t2[rcen]=t2_r; delta[rcen] = delta_r;
# interval-censored part
intcen = (1:n)[-rcen];
t1_int=rep(NA, n2);t2_int=rep(NA, n2); delta_int=rep(NA, n2);
npois = rpois(n2, 2)+1;
for(i in 1:n2){
  gaptime = cumsum(rexp(npois[i], 1));
  pp = Fioft(gaptime, X[intcen[i],], vn[intcen[i]]);
  ind = sum(u[intcen[i]]>pp);
  if (ind==0){
    delta_int[i] = 2;
    t2_int[i] = gaptime[1];
  }else if (ind==npois[i]){
    delta_int[i] = 0;
    t1_int[i] = gaptime[ind];
  }else{
    delta_int[i] = 3;
    t1_int[i] = gaptime[ind];
    t2_int[i] = gaptime[ind+1];
  }
}
t1[intcen]=t1_int; t2[intcen]=t2_int; delta[intcen] = delta_int;
## make a data frame
d = data.frame(t1=t1, t2=t2, X, delta=delta, tT=tT, ID=id, frail=v); table(d$delta)/n;

##----- Fit the PH model with variable selection -----##
# MCMC parameters
nburn=50000; nsave=10000; nskip=4; niter = nburn+nsave
mcmc=list(nburn=nburn, nsave=nsave, nskip=nskip, ndisplay=5000);
prior = list(maxL=15, a0=1, b0=1);
state <- list(cpar=1);
ptm<-proc.time()
res2 = survregbayes(formula = Surv(t1, t2, type="interval2")~x1+x2+x3+
x4+x5+frailtyprior("car", ID),
data=d, survmodel="PH", selection=TRUE, prior=prior, mcmc=mcmc, state=state,
dist="loglogistic", Proximity = W);
sfit2=summary(res2); sfit2;
systime2=proc.time()-ptm; systime2;
save.image(file="selection2.RData")

```

Note that the data have to be sorted by region ID before model fitting. The argument `mcmc` above specifies that the chain is subsampled every 5 iterates to get a total of 10,000 scans after a burn-in period of 50,000 iterations. The argument `prior` is used set all the priors; if nothing is specified, the default priors in the paper are used. The output is given below:

```

Posterior inference of regression coefficients
(Adaptive M-H acceptance rate: 0.03534):
Mean      Median      Std. Dev.  95%CI-Low  95%CI-Upp
x1   1.07285   1.07375   0.10060   0.88184   1.27191
x2   0.53212   0.96210   0.86665  -1.92366   1.18275
x3  -0.27420  -0.19516   1.00952  -2.20071   1.05240
x4  -0.06310  -0.04722   0.77375  -1.68505   1.47012
x5   0.02405  -0.02879   0.73981  -1.33391   1.52296

```

```

Posterior inference of precision parameter
(Adaptive M-H acceptance rate: 0.25684):
Mean      Median      Std. Dev.  95%CI-Low  95%CI-Upp

```

```
0.21172 0.19741 0.08665 0.08552 0.41521
```

Posterior inference of conditional CAR frailty variance

Mean	Median	Std. Dev.	95%CI-Low	95%CI-Upp
variance	0.7283	0.6891	0.2547	1.3430

Variable selection:

	x1,x2	x1,x2,x3	x1,x3	x1,x2,x5	x1,x2,x4	x1,x3,x5	x1,x2,x3,x4
prop.	0.4885	0.2173	0.1704	0.0374	0.0347	0.0154	0.0118

	x1,x2,x3,x5	x1,x3,x4	x1,x2,x4,x5	x1,x2,x3,x4,x5
prop.	0.0117	0.0088	0.0039	0.0001

Log pseudo marginal likelihood: LPML=-401.6587

Deviance Information Criterion: DIC=799.2814

Number of subjects: n=740

Remarks: The function `survregbayes` can also fit a semiparametric survival model (AFT, PH, or PO) with independent Gaussian frailties by setting `frailtyprior("iid", ID)`, with Gaussian random field frailties by setting `frailtyprior("grf", ID)`, a model without frailties by removing `frailtyprior()` in the formula, and a parametric (loglogistic, lognormal or weibull) survival model by specifying `a0` at a negative value and adding an argument `state=list(cpar=Inf)`. If FSA is used for GRF frailty models, the number of knots K and the number of blocks B are specified via `prior=list(nknots=K, nblock=B)`.

Appendix E Additional Results for Real Data Applications

E.1 Childhood Mortality Data in Nigeria

Table S1 reports several summary statistics for the childhood mortality data. Table S2 summarizes the results. The PO model significantly outperforms the AFT and PH as measured by both LPML and DIC. Regarding the regression coefficient estimates, we see that mother's age at birth, mother's BMI and child's gender child are all not statistically significant across the three models, and the residence of child is significant under the AFT and PO, but not under the PH. To choose a best set of risk factors, the variable selection algorithm is applied; the variable sets with the first three highest frequencies are shown in Table S3.

E.2 Loblolly Pine Survival Data

Table S4 presents some baseline characteristics for the trees.

Appendix F Additional Results for Simulations

F.1 Simulation I: Areal Data

Figure S1 presents the average, across the 500 MC replicates, of the fitted baseline survival functions and the results reveal that the proposed model is capable to capture complex baseline survival curves very well.

Table S1: Childhood mortality data. Summary statistics.

Continuous variables	Mean	Std. Dev.
Age at birth (yr.)	28.49	6.48
BMI	22.62	4.21
Breastfeed duration (mo.)	14.48	7.31
Preceding interval (mo.)	36.46	21.24
Categorical variables	Level	Proportion (%)
Censoring status	uncensored	1.67
	interval censored	7.54
	right censored	90.79
Place of delivery	hospital	32.78
	home/other	67.22
Gender of child	male	49.48
	female	50.52
Education	at least primary	47.26
	no education	52.74
place of residence	urban	34.82
	rural	65.18

Table S2: Childhood mortality data. Posterior means (95% credible intervals) of fixed effects β from fitting the AFT, PH and PO ICAR frailty models. The LPML and DIC are also shown for each model.

	AFT (LPML: -2127, DIC: 4250)	PH (LPML: -2126, DIC: 4235)	PO (LPML: -2079, DIC: 4153)
Age at birth	0.011(-0.005, 0.025)	0.014(-0.003, 0.030)	0.014(-0.004, 0.032)
BMI	0.008(-0.020, 0.035)	-0.001(-0.032, 0.028)	0.008(-0.024, 0.040)
Breastfeed	-0.262(-0.282,-0.243)	-0.266(-0.286,-0.246)	-0.357(-0.386,-0.328)
Preceding	-0.014(-0.021,-0.007)	-0.012(-0.018,-0.005)	-0.017(-0.024,-0.009)
Delivery	-0.428(-0.722,-0.139)	-0.445(-0.765,-0.141)	-0.542(-0.896,-0.194)
Gender	-0.057(-0.258, 0.131)	-0.085(-0.286, 0.128)	-0.074(-0.305, 0.156)
Education	-0.516(-0.773,-0.267)	-0.552(-0.828,-0.292)	-0.703(-1.022,-0.386)
Residence	-0.260(-0.511,-0.032)	-0.216(-0.486, 0.046)	-0.344(-0.642,-0.060)
τ^2	0.360(0.106, 0.860)	0.729(0.250, 1.609)	0.790(0.254, 1.973)

Table S3: Childhood mortality data. Selected first factors with high frequency.

Model	Proportions	Selected variables
AFT	0.447	Breastfeed, Preceding, Delivery, Education
	0.218	Breastfeed, Preceding, Delivery, Education, Residence
	0.100	Age at birth, Breastfeed, Preceding, Delivery, Education
PH	0.430	Breastfeed, Preceding, Delivery, Education
	0.125	Breastfeed, Preceding, Delivery, Education, Residence
	0.114	Age at birth, Breastfeed, Preceding, Delivery, Education
PO	0.318	Breastfeed, Preceding, Delivery, Education, Residence
	0.245	Breastfeed, Preceding, Delivery, Education
	0.101	Age at birth, Breastfeed, Preceding, Delivery, Education, Residence

Table S4: Loblolly pine data. Baseline characteristics of the 45,525 trees.

Categorical variables	Level	Proportion (%)
Censoring status	uncensored	12.65
	right censored	87.35
Treatment (treat)	1-control	24.78
	2-light thinning	40.32
	3-heavy thinning	34.90
Physiographic region (PhyReg)	1-coastal	55.53
	2-piedmont	37.01
	3-other	7.46
Crown class (C)	1-dominant	28.21
	2-codominant	52.22
	3-intermediate	15.50
	4-suppressed	4.07
Continuous variables	Mean	Std. Dev.
Total height of tree in meters (TH)	38.47	11.77
Diameter at breast height in cm (DBH)	5.88	1.77

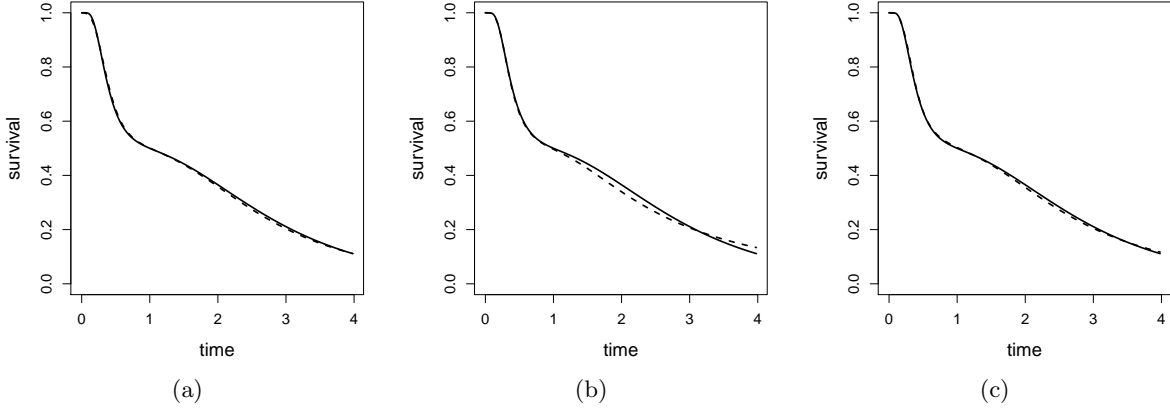


Figure S1: Simulated I. Mean, across the 500 MC replicates, of the posterior mean of the baseline survival functions under AFT (panel a), PH (panel b) and PO (panel c). The true curves are represented by continuous lines and the fitted curves are represented by dashed lines.

F.2 Simulation III: Georeferenced Data

We generated the data using the same settings as **Simulation I** except that $i = 1, \dots, 150, j = 1, \dots, 5$, and v_i follows the GRF prior with $\tau^2 = 1$, $\nu = 1$ and $\phi = 1$. The locations $\{\mathbf{s}_i\}_{i=1}^{150}$ were generated from $[0, 10]^2$ uniformly. Table S5 summaries the results, where we see that the point estimates of β are unbiased under all three models, SD-Est values are close to the corresponding PSDs, and the CP values are close to the nominal 95% level. We also observe that ϕ tends to be overestimated and the standard deviations for τ^2 and ϕ are underestimated (because SD-Est is smaller than PSD). Even though, the CP values are still close to 95%. The effective sizes for β are much smaller than these obtained for areal data, indicating that the georeferenced spatial dependency makes the posterior samples more correlated.

F.3 Simulation IV: Variable Selection

We next assess the performance of our variable selection method via three simulated examples. For each example, a data set was generated from the PH model with the $S_0(t)$ and ICAR setting the same as **Simulation I**. Under Example 1, we set $\mathbf{x}_{ij} = (x_{ij1}, \dots, x_{ij5})$ with $x_{ij1} \sim \text{Bernoulli}(0.5)$ and $x_{ij2}, \dots, x_{ij5} \stackrel{iid}{\sim} N(0, 1)$, and $\beta = (1, 1, 0, 0, 0)'$. Example 2 is identical to Example 1 except that $x_{ij3} = x_{ij2} + 0.15z$ where $z \sim N(0, 1)$, yielding a 0.989 correlation between x_2 and x_3 . For Example 3, we set $\mathbf{x}_{ij} = (x_{ij1}, \dots, x_{ij10})$ with $\beta = (1, 1, 1, 1, 1, 0, 0, 0, 0, 0)$ and $x_{ijk}|z \stackrel{iid}{\sim} N(z, 1)$ where $z \sim N(0, 1)$, which induces pairwise correlations of about 0.5. We applied our method to the three simulated datasets using all default priors designed for variable selection. A sample of 10,000 scans was thinned from 50,000 after a burn-in period of 10,000 iterations. Table S6 lists the proportions for the four highest frequency models under each example. The results reveal that our method predicts the right model very well even in the presence of extreme collinearity.

Table S5: Simulation III. Averaged bias (BIAS) and posterior standard deviation (PSD) of each point estimate, standard deviation (across 500 MC replicates) of the point estimate (SD-Est), coverage probability (CP) for the 95% credible interval, and effective sample size (ESS) for each point estimate.

Model	Parameter	BIAS	PSD	SD-Est	CP	ESS
AFT	$\beta_1 = 1$	-0.002	0.085	0.089	0.946	1933
	$\beta_2 = 1$	-0.000	0.045	0.042	0.964	1815
	$\tau^2 = 1$	0.000	0.329	0.220	0.948	548
	$\phi = 1$	0.082	0.388	0.357	0.962	471
PH	$\beta_1 = 1$	-0.016	0.112	0.116	0.934	1943
	$\beta_2 = 1$	-0.015	0.068	0.068	0.942	1110
	$\tau^2 = 1$	0.042	0.451	0.316	0.938	366
	$\phi = 1$	0.066	0.471	0.420	0.918	351
PO	$\beta_1 = 1$	-0.001	0.157	0.159	0.952	3006
	$\beta_2 = 1$	0.003	0.087	0.088	0.944	1960
	$\tau^2 = 1$	0.034	0.410	0.341	0.954	502
	$\phi = 1$	0.313	1.361	0.768	0.912	353

Table S6: Simulated IV. High frequency models with selected variables.

Example 1		Example 2		Example 3	
Variables	Proportions	Variables	Proportions	Variables	Proportions
1 2	0.80	1 2	0.49	1-5	0.63
1 2 3	0.08	1 2 3	0.22	1-5, 10	0.15
1 2 5	0.05	1 3	0.17	1-5, 7	0.09
1 2 4	0.05	1 2 5	0.04	1-5, 8	0.05

References

- Finley, A. O., Sang, H., Banerjee, S., and Gelfand, A. E. (2009). Improving the performance of predictive process modeling for large datasets. *Computational statistics & data analysis*, 53(8):2873–2884.
- Haario, H., Saksman, E., and Tamminen, J. (2001). An adaptive Metropolis algorithm. *Bernoulli*, 7(2):223–242.
- Han, C. and Carlin, B. P. (2001). Markov chain Monte Carlo methods for computing Bayes factors. *Journal of the American Statistical Association*, 96(455):1122–1132.
- Johnson, M. E., Moore, L. M., and Ylvisaker, D. (1990). Minimax and maximin distance designs. *Journal of statistical planning and inference*, 26(2):131–148.
- Kass, R. E. and Raftery, A. E. (1995). Bayes factors. *Journal of the american statistical association*, 90(430):773–795.
- Konomi, B. A., Sang, H., and Mallick, B. K. (2014). Adaptive Bayesian nonstationary modeling for large spatial datasets using covariance approximations. *Journal of Computational and Graphical Statistics*, 23:802–929.
- Sang, H. and Huang, J. Z. (2012). A full scale approximation of covariance functions for large spatial data sets. *Journal of the Royal Statistical Society: Series B (Statistical Methodology)*, 74(1):111–132.